NIST TECHNICAL NOTE 1677

Effect of Al_2O_3 Nanolubricant on a Passively Enhanced R134a Pool Boiling Surface with Extensive Measurement and Analysis Details

Mark A. Kedzierski

NIST National Institute of Standards and Technology • U.S. Department of Commerce

NIST TECHNICAL NOTE 1677

Effect of Al_2O_3 Nanolubricant on a Passively Enhanced Pool R134a Boiling Surface with Extensive Measurement and Analysis Details

Mark A. Kedzierski

U.S DEPARTMENT OF COMMERCE
National Institute of Standard and Technology
Building and Fire Research Laboratory
Building Environment Division
Gaithersburg, MD 20899-8631

September 2010

U.S. Department of Commerce
Gary F. Locke, Secretary

National Institute of Standards and Technology
Patrick D. Gallagher, Director

Effect of Al_2O_3 Nanolubricant on a Passively Enhanced R134a Pool Boiling Surface with Extensive Measurement and Analysis Details

M. A. Kedzierski
National Institute of Standards and Technology
Bldg. 226, Rm B114
Gaithersburg, MD 20899
Phone: (301) 975-5282
Fax: (301) 975-8973

ABSTRACT
This paper quantifies the influence of Al_2O_3 nanoparticles on the pool boiling performance of R134a/polyolester mixtures on a Turbo-BII-HP boiling surface. An Al_2O_3 nanolubricant (a lubricant containing dispersed nano-size particles) was made by suspending nominally 10 nm diameter Al_2O_3 particles in a synthetic polyolester to roughly a 1.0 % volume fraction. The nanoparticles caused, on average, a 12 % degradation in the boiling heat transfer relative to that for R134a/polyolester mixtures without nanoparticles for the three lubricant mass fractions that were tested. The degradation was nearly constant for heat fluxes between 20 kW/m^2 and 120 kW/m^2. It was speculated that the boiling heat transfer degradation was primarily due to (1) a combination of film boiling in the reentrant cavity rendering the nucleate boiling enhancement mechanism of the nanoparticles ineffective and (2) a reduction in bubble frequency due to the increased surface wetting as caused by the nanoparticles.

Keywords: additives, aluminum oxide, boiling, enhanced heat transfer, nanolubricant, nanotechnology, refrigerants, refrigerant/lubricant mixtures, structured surface

TABLE OF CONTENTS

ABSTRACT 4
Table of Contents 5
LIST of figures 5
List of tables 6
INTRODUCTION 7
APPARATUS 8
TEST SURFACE 8
MEASUREMENTS AND UNCERTAINTIES 8
EXPERIMENTAL RESULTS 9
DISCUSSION 12
CONCLUSIONS 13
ACKNOWLEDGEMENTS 14
NOMENCLATURE 15
English Subscripts 15
REFERENCES 16
APPENDIX A: UNCERTAINTIES 45

LIST OF FIGURES

Fig. 1 TEM of Al_2O_3 nanolubricant (Sarkas, 2009) 35
Fig. 2 Schematic of test apparatus 36
Fig. 3 OFHC copper flat test plate with Turbo-BII-HP surface and thermocouple coordinate system 37
Fig. 4 Photograph of Turbo-BII-HP surface 38
Fig. 5 Pure R134a boiling curve for Turbo-BII-HP surface 39
Fig. 6 R134a/RL68H mixtures boiling curves for Turbo-BII-HP surface 40
Fig. 7 Boiling heat flux of R134a/RL68H mixture relative to that of pure R134a for Turbo-BII-HP surface 41
Fig. 8 R134a/RL681AlO mixtures boiling curves for Turbo-BII-HP surface 42
Fig. 9 Boiling heat flux of R134a/RL68H1AlO mixtures relative to that of R134a/RL68H without nanoparticles for Turbo-BII-HP surface 43
Fig. 10 Mechanistic speculation of influence of nanoparticles on reentrant cavity bubble production 44
Fig. A.1 Expanded relative uncertainty in the heat flux of the surface at the 95 % confidence level 45
Fig. A.2 Expanded uncertainty in the temperature of the surface at the 95 % confidence level 46

LIST OF TABLES

Table 1 Conduction model choice **18**
Table 2 Pool boiling data **19**
Table 3 Number of test days and data points **31**
Table 4 Estimated parameters for cubic boiling curve fits for Turbo-BII-HP copper surface **32**
Table 5 Residual standard deviation of ΔT_s **33**
Table 6 Average magnitude of 95 % multi-use confidence interval for mean $T_w - T_s$ (K) **34**

INTRODUCTION

In recent years, nanofluids, i.e., liquids with dispersed nano-size particles, have been shown to be a potential means for enhancing the performance of chillers (Liu et al., 2009; Kedzierski, 2009). A major motivation for improving chiller performance is that energy efficiency is a primary component for net zero energy, high performance green building-design (OSTP 2008, EPA 2008). Chillers, that provide air conditioning for U.S. buildings, account for nearly 13 % of total building electric expenditures (EIA, 2008). Consequently, a cost-effective means for improving the efficiency of chillers would facilitate meeting green building goals.

Lubricant-based nanofluids, i.e., nanolubricants, can facilitate the stability of the nanoparticles in a refrigerant cycle while delivering them to the components of the cycle where they can produce the most benefit. Bi et al. (2007a) have shown that nanoparticles in compressor lubricant can improve its performance. Likewise, nanoparticles in the lubricant excess layer that covers evaporator surfaces can interact with nucleating bubbles and cause a heat transfer enhancement (Kedzierski, 2009). The combined effects of nanoparticles on heat transfer and compressor performance were illustrated by Bi et al. (2007b) when they showed that nanolubricants produced energy savings of more than 25 % in domestic refrigerators. These preceding studies suggest that it is worthwhile to investigate the potential benefits of nanolubricants for chillers.

Kedzierski (2010) showed that aluminum oxide (Al_2O_3) nanolubricants can improve the refrigerant boiling heat transfer of a 2 % by mass mixture on a smooth surface, on average, by roughly 150 % for heat fluxes less than 40 kW/m^2. The purpose of the present investigation was to determine if similar boiling heat transfer improvements could be obtained for a passively enhanced (structure) boiling surface. In order to investigate the influence of nanoparticle properties on refrigerant/lubricant pool boiling on a passively enhanced surface, the boiling heat transfer of three R134a/nanolubricant mixtures on a horizontal, flat, copper (Turbo-BII-HP)[1] surface were measured. A commercial polyolester lubricant (RL68H) with a nominal kinematic viscosity of 72.3 $\mu m^2/s$ at 313.15 K was the base lubricant that was mixed with nominally 10 nm diameter Al_2O_3 nanoparticles. Al_2O_3 nanoparticles have the advantages of a well-established, successful dispersion technology and being relatively inert with respect to lubricated compressor parts.

A manufacturer used a proprietary surfactant at a mass between 15 % and 20 % of the mass of the Al_2O_3 as a dispersant for the RL68H/Al_2O_3 mixture (nanolubricant). The manufacturer made the mixture such that 25 % of the mass was Al_2O_3 particles. The mixture was diluted in-house to a 3.6 % mass fraction of Al_2O_3 by adding neat RL68H and ultrasonically mixing the solution for approximately 24 h. A Dynamic Light Scattering (DLS) technique was used to measure the average nanoparticle size on a number basis. The diameter of most of the particles was approximately 10 nm (10.1 nm ± 1.3 nm) and the particles were well dispersed (Kedzierski, 2010). Figure 1 shows a Transmission Electron Microscopy (TEM) image of

[1] Certain commercial equipment, instruments, or materials are identified in this paper in order to specify the experimental procedure adequately. Such identification is not intended to imply recommendation or endorsement by the National Institute of Standards and Technology, nor is it intended to imply that the materials or equipment identified are necessarily the best available for the purpose.

the nanoparticles as taken by Sarkas (2009). The image confirms the good dispersion and shows that the particles are spherical with most of them having diameters of approximately 10 nm or less and a few having diameters close to 50 nm.

The mass faction was chosen so that it matched the nanoparticle mass fraction of the RL68H/Al_2O_3 study on a roughened, flat surface (Kedzierski, 2009). The RL68H/Al_2O_3 (99/1) volume fraction[2] mixture, a.k.a. RL68H1AlO, was mixed with pure R134a to obtain three R134a/RL68H1AlO mixtures at nominally 0.5 %, 1 %, and 2 % mass fractions for the boiling tests. In addition, the boiling heat transfer of three R134a/RL68H mixtures (0.5 %, 1 %, and 2 % mass fractions), without nanoparticles, was measured to serve as a baseline for comparison to the RL68H1AlO mixtures.

APPARATUS

Figure 2 shows a schematic of the apparatus that was used to measure the pool boiling data of this study. More specifically, the apparatus was used to measure the liquid saturation temperature (T_s), the average pool-boiling heat flux (q''), and the wall temperature (T_w) of the test surface. The three principal components of the apparatus were the test chamber, the condenser, and the purger. The internal dimensions of the test chamber were 25.4 mm × 257 mm × 1.54 m. The test chamber was charged with approximately 7 kg of refrigerant, giving a liquid height of approximately 80 mm above the test surface. As shown in Fig. 2, the test section was visible through two opposing, flat 150 mm × 200 mm quartz windows. The bottom of the test surface was heated with high velocity (2.5 m/s) water flow. The vapor produced by liquid boiling on the test surface was condensed by the brine-cooled, shell-and-tube condenser and returned as liquid to the pool by gravity. Further details of the test apparatus can be found in Kedzierski (2002) and Kedzierski (2001a).

TEST SURFACE

Figure 3 shows the oxygen-free high-conductivity (OFHC) copper flat test plate used in this study. The test plate was machined out of a single piece of OFHC copper by electric discharge machining (EDM). The internal fins of a commercial 25 mm (outer-diameter) Turbo-BII-HP tube were removed by EDM. The tube was then cut axially, annealed, flattened, and soldered onto the top of the test plate. Figure 4 shows a photograph of the fin surface. The Turbo-BII-HP surface has approximately 1660 fins per meter (fpm) oriented along the short axis of the plate. The overall height and root-width of a fin are 0.75 mm and 0.28 mm, respectively.

MEASUREMENTS AND UNCERTAINTIES

The standard uncertainty is the positive square root of the estimated variance. The individual standard uncertainties are combined to obtain the expanded uncertainty (U), which is calculated from the law of propagation of uncertainty with a coverage factor. All measurement uncertainties are reported at the 95 % confidence level except where specified otherwise. For the sake of brevity, only a summary of the basic measurements and uncertainties is given below. Complete detail on the heat transfer measurement techniques and uncertainties can be found in Kedzierski (2000) and Appendix A, respectively.

[2] The equivalent mixture is RL68H/Al_2O_3 (96.4/3.6) in terms of mass.

All of the copper-constantan thermocouples and the data acquisition system were calibrated against a glass-rod standard platinum resistance thermometer (SPRT) and a reference voltage to a residual standard deviation of 0.005 K. Considering the fluctuations in the saturation temperature during the test and the standard uncertainties in the calibration, the expanded uncertainty of the average saturation temperature was no greater than 0.04 K. Consequently, it is believed that the expanded uncertainty of the temperature measurements was less than 0.1 K.

Twenty 0.5 mm diameter thermocouples were force fitted into the wells of the side of the test plate shown in Fig. 3. The heat flux and the wall temperature were obtained by regressing the measured temperature distribution of the block to the governing two-dimensional conduction equation (Laplace equation). In other words, rather than using the boundary conditions to solve for the interior temperatures, the interior temperatures were used to solve for the boundary conditions following a backward stepwise procedure given in Kedzierski (1995)[3]. As shown in Fig. 3, the origin of the coordinate system was centered on the surface with respect to the y-direction at the heat transfer surface. Centering the origin in the y-direction reduced the uncertainty of the wall heat flux and temperature calculations by reducing the number of fitted constants involved in these calculations.

Fourier's law and the fitted constants from the Laplace equation were used to calculate the average heat flux (q'') normal to and evaluated at the heat transfer surface based on its projected area. The average wall temperature (T_w) was calculated by integrating the local wall temperature (T). The wall superheat was calculated from T_w and the measured temperature of the saturated liquid (T_s). Considering this, the relative expanded uncertainty in the heat flux ($U_{q''}$) was greatest at the lowest heat fluxes, approaching 8 % of the measurement near 20 kW/m^2. In general, the $U_{q''}$ remained approximately between 3 % and 6 % for heat fluxes greater than 50 kW/m^2. The average random error in the wall superheat (U_{Tw}) remained between 0.04 K and 0.12 K. Plots of $U_{q''}$ and U_{Tw} versus heat flux can be found in Appendix A.

EXPERIMENTAL RESULTS

The heat flux was varied between approximately 10 kW/m^2 and 140 kW/m^2 to simulate a range of possible operating conditions for R134a chillers. All pool-boiling measurements were made at 277.6 K saturated conditions. The data were recorded consecutively starting at the largest heat flux and descending in intervals of approximately 4 kW/m^2. The descending heat flux procedure minimized the possibility of any hysteresis effects on the data, which would have made the data sensitive to the initial operating conditions. Table 2 presents the measured heat flux and wall superheat for all the data of this study. Table 3 gives the number of test days and data points for each fluid. A total of 2108 measurements were made over 46 days.

The mixtures were prepared by charging the test chamber (see Fig. 2) with pure R134a to a known mass. Next, a measured mass of nanolubricant or lubricant was injected with a syringe through a port in the test chamber. The refrigerant/lubricant solution was mixed by

[3] Table 1 provides functional forms of the Laplace equation that were used in this study in the same way as was done in Kedzierski (1995) and in similar studies by this author.

flushing pure refrigerant through the same port where the lubricant was injected. All compositions were determined from the masses of the charged components and are given on a mass fraction basis. The maximum uncertainty of the mass fraction measurement is approximately 0.02 %, e.g., the range of a 2.0 % mass fraction is between 1.98 % and 2.02 %. Nominal or target mass compositions are used in the discussion. For example, the "actual" mass composition of the RL68H in the R134a/ RL68H (99.5/0.5) mixture was 0.50 % ± 0.02 %. Likewise, the RL68H mass fractions for R134a/ RL68H (99/1) and the R134a/ RL68H (98/2) mixtures were 1.00 % ± 0.02 % and 1.99 % ± 0.02 %, respectively. Using the same uncertainties, the nanolubricant mass fractions as tested with R134a were 0.50 %, 0.99 %, and 2.00 %.

Figure 5 is a plot of the measured heat flux (q") versus the measured wall superheat (T_w - T_s) for pure R134a pool boiling on the Turbo-BII-HP surface at a saturation temperature of 277.6 K. These measurements serve as a baseline for comparison to the refrigerant/pure-lubricant measurements. The open triangles represent the measured data while the solid line is a cubic best-fit regression or estimated means of the data. Six days of boiling pure R134a produced 252 measurements over a period of nearly two weeks. Two of the 252 R134a/RL68H (99.5/0.5) measurements were removed before fitting because they were identified as "outliers" based on having both high influence and high leverage (Belsley et al., 1980). The data sets for each test fluid presented in this manuscript exhibited a similar number of outliers and were regressed in the same manner. Table 4 gives the constants for the cubic regression of the superheat versus the heat flux for all of the fluids tested here. The residual standard deviation of the regressions – representing the proximity of the data to the mean – are given in Table 5. The dashed lines to either side of the mean represent the lower and upper 95 % simultaneous (multiple-use) confidence intervals for the mean. From the confidence intervals, the expanded uncertainty of the estimated mean wall superheat was, on average, 0.07 K. Table 6 provides the average magnitude of 95 % multi-use confidence interval for the fitted wall superheat for all of the test data.

Two long-dashed lines in Fig. 5 compare measurements of other studies to the present study. The R134a pool boiling curve of Chen and Tuzla (1996) on a 19 mm OD Turbo-BII-HP tube at T_s = 277.6 K crosses the present measured mean at a superheat of approximately 2.6 K. The maximum deviation between the present measured mean and the Chen and Tuzla (1996) boiling curve is 0.6 K, while the average absolute deviation is less than 0.2 K. The R134a boiling curve of Kedzierski (2001b) for a Turbo-BII-HP surface on a flat plate crosses the present measured mean superheat at approximately 1.4 K. For the same heat flux range as the Chen and Tuzla (1996) boiling curve, the average absolute deviation of the Kedzierski (2001b) curve from the present mean curve is less than 0.4 K. It is believed that the above comparisons validate the present measurements.

Figure 6 is a plot of the measured heat flux (q") versus the measured wall superheat (T_w - T_s) for the refrigerant/pure-lubricant mixtures at a saturation temperature of 277.6 K. The refrigerant/pure-lubricant measurements serve as the baseline for comparison to the refrigerant/nanolubricant pool boiling measurements. Twenty boiling curves were measured over the span of approximately two months. The open circles, squares, and stars represent the measured heat flux (q") versus the measured wall superheat (T_w - T_s) at a saturation

temperature of 277.6 K for the R134a/RL68H (99.5/0.5), R134a/RL68H (99/1), and R134a/RL68H (98/2) mixtures, respectively. From the 95 % multi-use confidence intervals, the expanded uncertainty of the estimated mean wall superheat was, on average, 0.09 K.

A general overview of the effect that the variation in the pure lubricant mass fraction has on R134a/lubricant pool boiling on the Turbo-BII-HP surface can be obtained from Fig. 6. Comparison of the three mean boiling curves shows that the superheats are within approximately 0.8 K of each other for the entire tested heat flux range. For the most part, the superheat for the refrigerant/lubricant mixtures is 0.3 K to 2.0 K greater than that for pure R134a indicating a heat transfer degradation with respect to pure R134a. Kedzierski (2001b) has shown that, in general, degradations associated with increased lubricant mass fractions occur when the concentration-induced bubble size reduction, and its accompanying loss of vapor generation per bubble, is not compensated by an increase in site density. Typically, heat transfer degradations have been observed to increase with respect to increasing lubricant mass fraction. The present measurements are consistent with this heat transfer performance trend for heat fluxes less than approximately 67 kW/m^2. At a heat flux of approximately 67 kW/m^2, the (98/2) mixture boiling curve crosses over the (99/1) mixture and the (99.5/0.5) mixture boiling curves, providing better boiling performance than either the (99/1) mixture or the (99.5/0.5) mixture for heat fluxes larger than 92 kW/m^2.

A more precise comparison of the R134a/RL68H heat transfer performances relative to pure R134a is given in Fig. 7. Figure 7 plots the ratio of the R134a/RL68H mixture heat flux to the pure R134a heat flux (q''_{PL}/q''_p) versus the pure R134a heat flux (q''_p) at the same wall superheat. Figure 7 illustrates the influence of lubricant mass fraction on the R134a/RL68H boiling curve with solid and dashed lines representing the mean heat flux ratios for each mixture and shaded regions showing the 95 % multi-use confidence level for each mean. A heat transfer degradation exists where the heat flux ratio is less than one and the 95 % simultaneous confidence intervals (depicted by the shaded regions) do not include the value one. For all compositions, the lubricant has caused a heat transfer degradation relative to the mean heat transfer of pure R134a for all measured q''_p. For the most part, the mean refrigerant/lubricant pool boiling heat flux resides between roughly 99 % and 60 % of that of the pure refrigerant. The heat flux ratio (q''_{PL}/q''_p) for all of the mixtures decreased slightly with respect to increasing heat flux for heat fluxes greater than 30 kW/m^2. The average heat flux ratio for each mixture between 30 kW/m^2 and 100 kW/m^2 was: 0.86, 0.75, and 0.71 for the R134a/RL68H (99.5/0.5), the R134a/RL68H (99/1), and the R134a/RL68H (98/2) mixtures, respectively. The minimum heat flux ratio for each mixture (for confidence intervals that do not include the value one) is shown in Fig. 7 and occurred for heat fluxes greater than 100 kW/m^2: 0.80 ± 0.02, 0.72 ± 0.02, and 0.69 ± 0.06 for the R134a/RL68H (99.5/0.5), the R134a/RL68H (99/1), and the R134a/RL68H (98/2) mixtures, respectively.

Figure 8 shows the measured heat flux (q'') versus the measured wall superheat (T_w - T_s) for three mixtures of R134a and the nanolubricant RL68H1AlO at a saturation temperature of 277.6 K. Twenty-two boiling curves were measured over the span of approximately five weeks. The closed circles, squares, and stars represent the measurements for the R134a/ RL68H1AlO (99.5/0.5), R134a/ RL68H1AlO (99/1), and R134a/ RL68H1AlO (98/2)

mixtures, respectively. From the 95 % multi-use confidence intervals, the expanded uncertainty of the estimated mean wall superheat was, on average, 0.17 K.

As Fig. 8 shows, a modest variation in the boiling performance is exhibited among the three nanofluids given the variation in composition. For example, the mean boiling curves of the refrigerant/nanolubricant mixtures differ by no more than 0.8 K. For heat fluxes less than 95 kW/m^2, the difference in superheat between the (99/1) mixture and the (98/2) mixture is less than 0.2 K. In this region, the boiling performance of the R134a/RL68H1AlO mixtures is ranked from best to worst as follows: (99.5/0.5), (99/1), and (98/2). The (98/2) nanolubricant mixture boiling curve exhibits the same crossover at approximately 67 kW/m^2 that was observed in Fig. 6 for the R134a/pure-lubricant mixtures.

Figure 9 summarizes the influence of Al_2O_3 nanoparticles on R134a/RL68H boiling heat transfer. The figure plots the ratio of the R134a/RL68H1AlO heat flux to the R134a/RL68H heat flux (q''_{Al}/q''_{PL}) versus the R134a/RL68H mixture heat flux (q''_{PL}) at the same wall superheat for the Turbo-BII-HP surface. The three different compositions are represented by three solid lines where each R134a/nanolubricant mixture is compared to the R134a/pure-lubricant mixture at the same mass fraction. Although the mean heat flux ratio for the (99/1) mixture is greater than one for heat fluxes less than 14 kW/m^2, neither an enhancement nor a degradation can be claimed in this region because the confidence intervals include the value one. Similarly, the confidence intervals show that the nanoparticles have caused a relatively constant heat transfer degradation compared to the boiling of the R134a/RL68H mixtures (without nanoparticles), for heat fluxes greater than 20 kW/m^2. The average heat flux ratio for heat fluxes greater than 20 kW/m^2 is approximately 0.87, 0.89, and 0.89 for the 0.5 %, the 1 %, and the 2 % nanolubricant mass fractions, respectively. Consequently, the nanolubricant mass fraction had little influence on the magnitude of the heat transfer degradation.

DISCUSSION

Figure 10 is used to illustrate why a nanolubricant with twice the nanoparticle volume fraction significantly enhance R134a boiling on a smooth surface (Kedzierski, 2010a), but caused a roughly 12 % degradation for the Turbo-BII-HP reentrant cavity surface. The schematic shows the Turbo-BII-HP fin in cross section revealing its cavity with a mouth radius of r_c. The nanolubricant excess layer is shown, roughly to scale, being approximately 40 μm thick (Kedzierski, 2002) on the approximately 0.7 mm high fin. Kedzierski (2010) proposed that the enhancement caused by the nanolubricant for a smooth boiling surface was due to surface work on bubbles as caused by momentum transfer between growing bubbles and nanoparticles suspended within the lubricant excess layer. It is proposed here that the momentum transfer between bubbles and particles still occurs for reentrant cavities; however, thin film evaporation into large seed bubbles in the reentrant cavity suppresses the nucleate boiling in the nanolubricant excess layer, thus, reducing the interaction between nanoparticles and bubbles in the nanolubricant excess layer.

Arshad and Thome (1983) show that thin film evaporation primarily governs the heat transfer within reentrant cavities. Because of this, bubble nucleation at the wall is likely to be reduced, and thus, have less influence on the overall heat-transfer. Being that the

nanoparticles enhance boiling heat transfer via momentum transfer between nanoparticles and bubbles during bubble growth from the wall, the enhancement effect of the nanoparticles is minimized for reentrant cavity boiling. For reentrant cavities, the boiling is controlled primarily by the cavity geometry, including the size of its opening and the contact angle that the bubble makes at the cavity mouth (Griffith and Wallis, 1960; Chien and Webb, 1998). In addition, Gerardi et al. (2010) have shown that nanoparticles can cause increased surface wetting, i.e., reduced contact angle, which leads to a small bubble departure frequency. A reduced bubble frequency could explain the approximately 12 % heat transfer degradation exhibited by the refrigerant/nanolubricant boiling on the Turbo-BII-HP surface.

No white deposits were visible on the boiling surface after test, suggesting that the lubricant excess layer was successful at suspending the Al_2O_3 nanoparticles above the surface and, thus, limiting the number that become lodged in the surface cavities. For this reason, one would think that any heat transfer degradation that could have been attributed to nanoparticles filling surface cavities would have been compensated for by the heat transfer enhancement as caused by nanoparticles in the lubricant excess layer. However, the question remains if there were enough particles in the excess layer to cause an enhancement. Such a critical nanoparticle volume fraction for obtaining boiling improvement was observed for the smooth surface (Kedzierski, 2009). The enhanced surface, because of its larger surface area, may require a larger nanoparticle volume fraction in the lubricant than the smooth surface, and larger than what was tested here, to obtain an enhancement in boiling.

Future research is required to determine if a nanoparticle mass fraction larger than 3.6 % is required to improve reentrant cavity surfaces. In addition, future research is required to determine if nanolubricants can be used to improve the boiling heat transfer performance of open structured surfaces such as the trapezoidal fin. The boiling performance of open surfaces is more likely to be strongly influenced by nucleate boiling within the lubricant excess layer and, in return, benefit from nanoparticles.

CONCLUSIONS

The effect of Al_2O_3 nanoparticles on the boiling performance of R134a/polyolester mixtures on a flattened, horizontal Turbo-BII-HP surface was investigated. A nanolubricant containing roughly 10 nm diameter Al_2O_3 nanoparticles at 1.0 % volume fraction with a polyolester lubricant was mixed with R134a at three different mass fractions. Even though a previous study had shown significant enhancements for a plain surface, the Al_2O_3 nanoparticles caused a heat transfer degradation relative to the heat transfer of pure R134a/polyolester for all three of lubricant mass fractions on the Turbo-BII-HP surface. For all nanolubricant mass fractions with refrigerant, the degradation in heat flux was approximately 12 % and nearly independent of superheat. The average heat flux degradation for heat fluxes larger than 20 kW/m^2 was approximately 13 %, 11 %, and 11 % for the 0.5 %, the 1 %, and the 2 % mass fractions, respectively.

It was speculated that the boiling heat transfer degradation was primarily due to a combination of film boiling in the reentrant cavity rendering the nucleate boiling enhancement mechanism of the nanoparticles ineffective and a reduction in bubble frequency due to the increased surface wetting caused by the nanoparticles.

ACKNOWLEDGEMENTS
This work was jointly funded by NIST and the U.S. Department of Energy (project no. DE-EE0002057/004) under Project Manager Antonio Bouza. Thanks go to D. Flynn of NIST personnel for his constructive criticism of the first draft of the manuscript. Thanks go to D. Han of Ohio Carbon Bank for his constructive criticism of the second draft of the manuscript. Furthermore, the author extends appreciation to W. Guthrie and A. Heckert of the NIST Statistical Engineering Division for their consultations on the uncertainty analysis. Boiling heat transfer measurements were taken by D. Wilmering of KT Consulting at the NIST laboratory. The RL68H (EMKARATE RL 68H) was donated by K. Lilje of CPI Engineering Services, Inc. The RL68H1AlO was manufactured by Nanophase Technologies with an aluminum oxide and dispersant in RL68H especially for NIST.

NOMENCLATURE

English Symbols

A_n	regression constant in Table 4 n=0,1,2,3
q"	average wall heat flux, $W \cdot m^{-2}$
r_c	radius of cavity opening, m
T	temperature, K
T_w	temperature at roughened surface, K
U	expanded uncertainty
X	model terms given in Table 2

English Subscripts

Al	nanolubricant
p	pure R134a
PL	refrigerant/pure lubricant (R134a/RL68H) mixture
q"	heat flux
s	saturated state
Tw	wall temperature

REFERENCES

Arshad, J., and Thome, J. R., 1983, “Enhanced Boiling Surfaces: Heat Transfer Mechanism and Mixture Boiling,” ASME/JSME Joint Thermal Engineering Conference, Honolulu, Vol. 1, pp. 191-197.

Belsley, D. A., Kuh, E., and Welsch, R. E., 1980, Regression Diagnostics: Identifying Influential Data and Sources of Collinearity, New York: Wiley.

Bi, S., Shi, L., and Zhang, L., 2007a, “Performance Study of a Domestic Refrigerator Using R134a/Mineral Oil/Nano-TiO_2 as Working Fluid,” *Proceedings of International Conference of Refrigeration,* Beijing, ICRO7-B2-346.

Bi, S., Shi, L., and Zhang, L., 2007b, “Application of Nanoparticles in Domestic Refrigerators,” Applied Thermal Engineering, Vol. 28, pp. 1834-1843.

Chien, L. H., and Webb, R. L., 1998, “A Nucleate Boiling Model for Structured Enhanced Surfaces,” Int. J. Heat Mass Transfer, Vol. 41, No. 14, pp. 2183-2195.

Chen, J., and Tuzla, K., 1996, "Heat Transfer Characteristics of Alternative Refrigerants; Volume 3: Condenser and Evaporator Outside Tube," EPRI TR-106016-V3, project 3412-53, Palo Alto.

Energy Information Administration (EIA), 2008, “2003 Commercial Buildings Energy Consumption Survey: Consumption and Expenditures Tables,” http://www.eia.doe.gov/emeu/cbecs/cbecs2003/detailed_tables_2003/2003set15/2003pdf/c13a.pdf (January 2009).

Environmental Protection Agency (EPA), 2008, “EPA Green Building Strategy,” EPA-100-F-08-073.

Gerardi C., Buongiorno, J., Hu, L. W., and McKrell, T., 2010. “Infrared Thermometry Study of Nanofluid Pool Boiling Phenomena,” accepted for publication in HKIE Transactions.

Griffith, P., and Wallis, J. D., 1960, “The Role of Surface Conditions in Nucleate Boiling, *Chem. Eng. Prog. Symp. Ser.*, Vol. 56, No. 49, pp. 49-63.

Kedzierski, M. A., 2010, “Effect of Al2O3 Nanolubricant on R134a Pool Boiling Heat Transfer with Extensive Measurement and Analysis Details,” NIST Technical Note 1663, U.S. Department of Commerce, Washington, D.C.

Kedzierski, M. A., 2009, “Effect of CuO Nanoparticle Concentration on R134a/Lubricant Pool-Boiling Heat Transfer," ASME J. Heat Transfer, Vol. 131, No. 4, 043205.

Kedzierski, M. A., 2002, “Use of Fluorescence to Measure the Lubricant Excess Surface Density During Pool Boiling,” Int. J. Refrigeration, Vol. 25, pp. 1110-1122.

Kedzierski, M. A., 2001a, “Use of Fluorescence to Measure the Lubricant Excess Surface Density During Pool Boiling,” NISTIR 6727, U.S. Department of Commerce, Washington, D.C.

Kedzierski, M. A., 2001b, “The Effect of Lubricant Concentration, Miscibility and Viscosity on R134a Pool Boiling” Int. J. Refrigeration, Vol. 24, No. 4., pp. 348-366.

Kedzierski, M. A., 2000, “Enhancement of R123 Pool Boiling by the Addition of Hydrocarbons,” Int. J. Refrigeration, Vol. 23, pp. 89-100.

Kedzierski, M. A., 1995, “Calorimetric and Visual Measurements of R123 Pool Boiling on Four Enhanced Surfaces,” NISTIR 5732, U.S. Department of Commerce, Washington.

Liu, M. S., Lin, M.C.C., Liaw, J.S., Hu, R. Wang, C.C., 2009, “Performance Augmentation of a Water Chiller System Using Nanofluids,” Proceedings of ASHRAE Winter Conference, Chicago, CH-09-058.

Office of Science and Technology Policy (OSTP), 2008, “Federal Research and Development Agenda for Net-Zero Energy, High-Performance Green Buildings,” National Science and Technology Council Committee on Technology, http://www.ostp.gov/galleries/NSTC%20Reports/FederalRDAgendaforNetZeroEnergyHighPerformanceGreenBuildings.pdf (March 2009).

Sarkas, H., 2009, Private Communications, Nanophase Technologies Corporation, Romeoville, IL.

Table 1 Conduction model choice

X_0= constant (all models) X_1= x X_2= y X_3= xy $X_4=x^2-y^2$ $X_5= y(3x^2-y^2)$ $X_6= x(3y^2-x^2)$ $X_7= x^4+y^4-6(x^2)y^2$ $X_8= yx^3-xy^3$	
Fluid	Most frequent models
Pure R134a (file: 134TB09.dat)	X_1,X_2,X_5 (117 of 250) 47 % X_1,X_2,X_4,X_5 (51 of 250) 20 % X_1,X_5,X_8 (45 of 250) 18 %
R134a/RL68H (99.5/0.5) (file: RL685TB.dat)	X_1,X_2,X_4,X_5,X_6 (135 of 320) 42 % X_1,X_2,X_5 (63 of 320) 20 % X_1,X_5,X_8 (46 of 320) 14 % X_1,X_2,X_4,X_5 (39 of 320) 12 %
R134a/RL68H (99/1) (file: RL681TB.dat)	X_1,X_2,X_4,X_5,X_6 (92 of 282) 33 % X_1,X_3,X_4,X_6 (56 of 282) 20 % X_1,X_2,X_5 (41 of 282)15 % X_1,X_2,X_4,X_5 (28 of 320) 9 %
R134a/RL68H (98/2) (file: RL682TB.dat)	X_1,X_3,X_4,X_6 (106 of 337) 31 % X_1,X_2,X_5 (74 of 337) 22 % X_1,X_2 (45 of 337) 13 % X_1,X_2,X_4,X_6 (41 of 337) 12 %
R134a/RL681AlO (99.5/0.5) (file: TBAl5.dat)	X_1,X_2,X_3,X_4,X_6 (81 of 285) 28 % X_1,X_3,X_4,X_6 (73 of 285) 26 % X_1,X_2,X_5 (57 of 285) 20 % X_1,X_2,X_4,X_5 (51 of 285) 18 %
R134a/RL681AlO (99/1) (file: TBAl1.dat)	X_1,X_2,X_3,X_4 (100 of 330) 30 % X_1,X_5 (67 of 330) 20 % X_1,X_2,X_3 (45 of 330) 14 % X_1,X_5,X_8 (41 of 330) 12 %
R134a/RL681AlO (98/2) (file: TBAl2.dat)	X_1,X_2,X_3 (112 of 264) 42 % X_1,X_5 (61 of 264) 23 % X_1,X_5,X_8 (52 of 264) 20 % X_1,X_2,X_5 (25 of 264) 9 %

Table 2 Pool boiling data

Pure R134a
File: 134TB09.dat

ΔT_s (K)	q'' (W/m^2)
5.94	124988.
5.86	128189.
5.84	127893.
5.53	119161.
5.46	117874.
5.46	117607.
5.22	111123.
5.21	110940.
5.19	110858.
4.92	103874.
4.91	103643.
4.92	103766.
4.45	92287.
4.45	92050.
4.44	91924.
4.15	85908.
4.13	85872.
4.13	85962.
3.61	76541.
3.61	76493.
3.64	76835.
3.10	69116.
3.09	68898.
3.08	69105.
2.61	61271.
2.61	61331.
2.61	61284.
2.18	54240.
2.19	54435.
2.20	54681.
1.72	46931.
1.69	46494.
1.72	46972.
1.30	39583.
1.31	39570.
1.34	39980.
0.91	32054.
0.91	31317.
0.88	30995.
0.54	24583.
0.52	24299.
5.71	115768.
5.72	116229.
5.66	120436.
5.27	110404.
5.27	110299.
5.27	110182.
4.94	102361.
4.93	102557.
4.97	103194.
4.53	92739.
4.54	92962.
4.57	94551.
4.13	83267.
4.13	83429.
4.13	83573.
3.65	75688.
3.64	75574.
3.67	75812.
3.16	68515.
3.19	68801.
3.21	69072.
2.66	60500.
2.69	60970.
2.71	60795.
2.32	54719.
2.31	54182.
2.30	54587.
1.81	46337.
1.84	46653.
1.87	47172.
1.37	38862.
1.39	38837.
1.34	38230.
1.00	32372.
1.00	32510.
1.03	32826.
0.63	25034.
0.57	24007.
0.51	22900.
0.31	18664.
0.27	17974.
6.28	131692.
6.28	132533.
6.28	133340.
5.94	123501.
6.00	124957.
6.02	125662.
5.56	119213.
5.59	119889.
5.70	116324.
5.32	110417.
5.30	111426.
5.30	111390.
4.96	103108.
4.95	102632.
4.93	102217.
4.53	91297.
4.48	91970.
4.45	91306.
4.14	83145.
4.14	83057.
4.14	83116.
3.68	75691.
3.71	76382.
3.74	76768.
3.19	68516.
3.21	68829.
3.23	68942.
2.74	60774.
2.72	60700.
2.70	60452.
2.27	53466.
2.17	51988.
2.22	52788.
1.73	44798.
1.69	44318.
1.71	44399.
1.30	37500.
1.29	37052.
1.29	36804.
0.96	31185.
0.94	30965.
0.94	30893.
0.57	23938.
0.62	24858.
0.63	24464.
0.20	15611.
6.15	124092.
6.19	125686.
6.15	131238.
5.92	118632.
5.95	119821.
5.99	121027.
5.60	115553.
5.62	116065.
5.66	116886.
5.28	106856.
5.28	107249.
5.30	107876.
4.89	98058.
4.93	98340.
4.96	97348.
4.54	87890.
4.51	87645.
4.51	87494.
4.12	79508.
4.13	79613.
4.13	79670.
3.65	71134.
3.61	70590.
3.61	70614.
3.26	65613.
3.22	65320.
3.23	65318.
2.71	56495.
2.73	56877.
2.72	56883.
2.16	48679.
2.17	48925.
2.16	48720.
1.75	42365.
1.77	42641.
1.79	42692.
1.32	34611.
1.27	33701.
1.20	32845.
0.81	26730.
0.77	26408.
6.33	124178.
6.34	122559.
6.32	122444.
5.97	113148.
5.94	112863.
5.93	112882.
5.57	104314.
5.56	103915.
5.58	104288.
5.17	99018.
5.16	99189.
5.16	99258.

4.80	91022.
4.79	90890.
4.81	89510.
4.38	81226.
4.37	80888.
4.38	81146.
3.87	71673.
3.85	72285.
3.91	72913.
3.50	67001.
3.50	67015.
3.49	66897.
2.83	56545.
2.87	57218.
2.85	56597.
2.53	51518.
2.53	51667.
2.50	51131.
1.93	43431.
1.92	43305.
1.93	43477.
1.53	36434.
1.53	36494.
1.54	36475.
0.99	28749.
0.96	28423.
0.98	28366.
0.63	22809.
0.60	22119.
6.13	121711.
6.15	121847.
6.14	121436.
5.79	112185.
5.68	114656.
5.71	110507.
5.49	105278.
5.48	104999.
5.50	105609.
5.05	99304.
4.98	98676.
4.99	98828.
4.62	89021.
4.62	88952.
4.63	88976.
4.28	81954.
4.23	81470.
4.23	81256.
3.86	74446.
3.84	74520.
3.87	74907.
3.31	66903.
3.33	67214.
3.34	67494.
2.85	59593.
2.80	58958.
2.87	59581.
2.24	50907.
2.29	51592.
2.28	51269.
1.81	44472.
1.80	44432.
1.81	44485.
1.35	37394.
1.34	37048.
1.36	37072.
1.00	31281.
0.92	30494.
0.89	30137.
0.52	23312.
0.50	22726.
0.48	22251.

R134a/RL68H (99.5/0.5)
File: RL685TB.dat

ΔT_s (K)	q'' (W/m^2)
7.34	123692.
7.39	127157.
7.44	128202.
7.02	117309.
7.07	116745.
7.10	117171.
6.71	110097.
6.74	110353.
6.79	110925.
6.32	101271.
6.39	101024.
6.43	101418.
6.03	93629.
6.04	93344.
6.07	93696.
5.64	85431.
5.63	87584.
5.65	84894.
5.19	77244.
5.18	79339.
5.19	76923.
4.68	71071.
4.61	70266.
4.61	70149.
4.18	62705.
4.12	62055.
4.14	62209.
3.56	54716.
3.47	54329.
3.46	54151.
2.84	48873.
2.83	48711.
2.90	49494.
2.21	42228.
2.15	41640.
2.12	41231.
1.60	35195.
1.48	34107.
1.43	33613.
0.93	27591.
0.91	27381.
0.92	27392.
0.54	22089.
0.53	21734.
0.52	21469.
0.12	12926.
0.14	11868.
7.45	123047.
7.48	123792.
7.51	124849.
7.01	116001.
7.07	116680.
7.11	116809.
6.59	107839.
6.61	107877.
6.71	108718.
6.25	100131.
6.28	100300.
6.33	100668.
5.85	92069.
5.85	92099.
5.89	92510.
5.43	84394.
5.45	84354.
5.47	84626.
4.90	75462.
4.91	75094.
4.89	74912.
4.45	70889.
4.43	70593.
4.45	70625.
3.92	62023.
3.94	62258.
3.92	61960.
3.28	54628.
3.18	53608.
3.18	53553.
2.71	49623.
2.68	49439.
2.72	49755.
2.11	42471.
2.07	42123.
2.06	41863.
1.39	34322.
1.32	33940.
1.29	33581.
0.90	27876.
0.88	27506.
0.87	27333.
0.53	21271.
0.48	20615.
0.48	20473.
0.17	14399.
0.18	13522.
7.32	122105.
7.32	122046.
7.29	121990.
6.85	114617.
6.82	113910.
6.80	113306.
6.39	106369.
6.38	105968.
6.37	105755.
5.96	97590.
5.93	96758.
5.93	96214.
5.54	89642.
5.54	89193.
5.51	88510.
5.10	80423.
5.12	80642.
5.17	81049.
4.65	73488.
4.62	73360.
4.65	73448.
4.08	68314.
4.08	68143.

4.09	68109.
3.61	59669.
3.63	59640.
3.61	61291.
2.96	52842.
2.92	52745.
2.98	53123.
2.50	48119.
2.52	48609.
2.51	48553.
1.83	40921.
1.74	40301.
1.86	41614.
1.26	34085.
1.23	33630.
1.28	33991.
0.75	25626.
0.73	25699.
0.74	25608.
0.37	19295.
0.33	18967.
0.34	18926.
0.13	13743.
0.16	12966.
7.14	119247.
7.25	121340.
7.38	124264.
7.00	117213.
7.06	118100.
7.15	119464.
6.57	109749.
6.59	110222.
6.65	111192.
6.18	101848.
6.16	101349.
6.18	101203.
5.73	92792.
5.69	92120.
5.68	91782.
5.25	84286.
5.25	83989.
5.25	83715.
4.72	75382.
4.75	75753.
4.81	76475.
4.44	72876.
4.33	71142.
4.35	69542.
3.91	63455.
3.93	63467.
3.92	63222.
3.12	53827.
3.05	54308.
3.04	53067.
2.63	49270.
2.58	48974.
2.57	48540.
2.04	42801.
1.99	42179.
1.97	41871.
1.37	34589.
1.30	34091.
1.33	34012.
0.82	27195.
0.79	26787.
0.77	26477.
0.45	20000.
0.36	19137.
0.37	18764.
7.39	128640.
7.38	128792.
7.36	128789.
6.92	120372.
6.93	121172.
6.97	121583.
6.54	113254.
6.54	113021.
6.53	112906.
6.21	106427.
6.22	106436.
6.23	106358.
5.77	96982.
5.77	96354.
5.77	95957.
5.32	87804.
5.31	87550.
5.31	87154.
4.96	81164.
5.00	81397.
5.05	82026.
4.47	73026.
4.52	73635.
4.57	74108.
3.98	68335.
3.91	67528.
3.99	68088.
3.42	59079.
3.38	58616.
3.32	57903.
2.75	52310.
2.74	52284.
2.72	52050.
2.19	45797.
2.20	45966.
2.21	46018.
1.60	38916.
1.64	39282.
1.66	39209.
1.07	31650.
0.99	31009.
0.99	30873.
0.60	24336.
0.60	24276.
0.62	24235.
0.23	16748.
0.20	16130.
7.12	122483.
7.05	121627.
7.04	121761.
6.67	114894.
6.66	114697.
6.71	115637.
6.31	108440.
6.36	108826.
6.40	109395.
5.90	100389.
5.92	99827.
5.94	100165.
5.48	91678.
5.48	91664.
5.48	91742.
5.02	84113.
5.00	83337.
5.02	83153.
4.58	78404.
4.54	77984.
4.56	77853.
4.12	69328.
4.12	69322.
4.09	68625.
3.62	62682.
3.49	60651.
3.37	60452.
2.95	55328.
2.97	55582.
3.03	56242.
2.39	49006.
2.41	49086.
2.47	49812.
1.86	42426.
1.88	42476.
1.85	42064.
1.19	33590.
1.13	33056.
1.12	32734.
0.75	27220.
0.73	26970.
0.71	26586.
0.43	20873.
0.42	20603.
0.41	20447.
0.13	13851.
0.11	13296.
7.23	130020.
7.09	127595.
6.92	124931.
6.56	117541.
6.52	117253.
6.58	117938.
6.23	110747.
6.26	110999.
6.30	111541.
5.83	102385.
5.83	102171.
5.85	102027.
5.37	93397.
5.36	93109.
5.38	93142.
4.96	86014.
4.97	88562.
5.00	88627.
4.42	77571.
4.44	77848.
4.43	77709.
3.99	71382.
3.98	71344.
3.97	71007.
3.55	65492.
3.54	65143.
3.50	65536.
2.87	57914.
2.81	57637.
2.88	58402.
2.28	50275.
2.31	50385.

2.31	50445.
1.72	43029.
1.66	42562.
1.66	42555.
1.19	36336.
1.18	35576.
1.14	34890.
0.67	27266.
0.62	26544.
0.74	28348.
0.41	21078.
0.41	21251.
0.42	21447.
0.15	14856.
0.13	14394.
0.12	14257.

R134a/RL68H (99/1)
File: RL681TB.dat

ΔT_s (K)	q'' (W/m^2)
7.12	122442.
7.10	123111.
7.11	124481.
6.74	114310.
6.77	114536.
6.81	115441.
6.66	110182.
6.66	110734.
6.67	110920.
6.32	101401.
6.30	101426.
6.34	101088.
5.99	93390.
6.00	93158.
6.00	93175.
5.63	85284.
5.59	85058.
5.61	84825.
5.11	76380.
5.09	76014.
5.10	78312.
4.68	71636.
4.69	69997.
4.70	71658.
4.19	62911.
4.14	62393.
4.14	62471.
3.54	55272.
3.59	55805.
3.69	56654.
2.82	49016.
2.81	48921.
2.84	49150.
2.23	42203.
2.19	41533.
2.15	41136.
1.62	35348.
1.57	34741.
1.47	33963.
0.56	20382.
7.56	132655.
7.56	133149.
7.54	133831.
7.29	125605.
7.29	125618.
7.31	126610.
7.04	117780.
7.07	118408.
7.08	118543.
6.76	108364.
6.77	107817.
6.75	107670.
6.50	100683.
6.49	100415.
6.47	99642.
6.08	90819.
6.14	91750.
6.15	92067.
5.71	83258.
5.68	82981.
5.62	81353.
5.26	75317.
5.28	75149.
5.36	76419.
4.78	68165.
4.84	71591.
4.90	69598.
4.19	62517.
4.30	63945.
4.34	64256.
3.67	54922.
3.60	54449.
3.58	53757.
2.98	48745.
2.94	48398.
2.99	48067.
2.28	40355.
2.20	39671.
2.20	39510.
1.67	33284.
1.58	32727.
1.55	32434.
1.08	26234.
1.07	26132.
1.06	25935.
0.67	19573.
0.61	18988.
0.59	18650.
0.13	10167.
7.41	135876.
7.40	135981.
7.38	136107.
7.09	127050.
7.09	126533.
7.07	126121.
6.79	118102.
6.77	117213.
6.80	117569.
6.51	108915.
6.51	109108.
6.54	109634.
6.22	101095.
6.23	100708.
6.24	100636.
5.88	92090.
5.89	91696.
5.87	91460.
5.52	83803.
5.49	83080.
5.47	82585.
5.07	75185.
5.02	74518.
5.01	74295.
4.55	66737.
4.50	66261.
4.50	68641.
4.07	62655.
4.04	62436.
4.08	62971.
3.44	53491.
3.44	53403.
3.45	53511.
2.81	47329.
2.80	47288.
2.82	47604.
2.26	40563.
2.20	40206.
2.19	40098.
1.67	33719.
1.61	33381.
1.61	33398.
1.06	26096.
1.03	25716.
1.00	25440.
0.57	18925.
0.56	18767.
0.55	18805.
0.27	13476.
7.55	131770.
7.53	131635.
7.43	129290.
7.24	122481.
7.28	123595.
7.29	124737.
6.95	114513.
6.97	115221.
6.99	115531.
6.66	105302.
6.65	104662.
6.64	104563.
6.33	96386.
6.35	96361.
6.34	96285.
6.03	88396.
5.94	86145.
5.85	84576.
5.61	79300.
5.64	79744.
5.67	80302.
5.16	71451.
5.19	71592.
5.17	71362.
4.55	65157.
4.50	62337.
4.46	64190.
4.01	58459.
3.97	58127.
3.94	57853.
3.30	50270.
3.29	49188.
3.28	49170.

2.79	44438.
2.73	44108.
2.71	44212.
2.12	37268.
2.05	36625.
2.04	36581.
1.49	29986.
1.44	29512.
1.41	29329.
0.97	23466.
0.94	23057.
0.92	22834.
0.54	17100.
0.47	16183.
0.45	15611.
0.12	9939.
7.54	124531.
7.53	125595.
7.54	126900.
7.30	119606.
7.29	119818.
7.32	120504.
7.09	112386.
7.10	112904.
7.12	113415.
6.81	104504.
6.82	104179.
6.82	104028.
6.47	94772.
6.47	94100.
6.47	93855.
6.16	87126.
6.15	86965.
6.16	86617.
5.80	79602.
5.75	78413.
5.71	77469.
5.32	70795.
5.25	69909.
5.25	69831.
4.80	63678.
4.73	62744.
4.72	62820.
4.35	60497.
4.29	57008.
4.33	60292.
3.68	50746.
3.62	49989.
3.64	50378.
3.08	44185.
3.05	43963.
3.06	43824.
2.41	38082.
2.39	38251.
2.42	38379.
1.81	31786.
1.81	31805.
1.78	31479.
1.22	24833.
1.17	24540.
1.17	24440.
0.71	17969.
0.65	17481.
0.66	17571.
0.31	11479.

7.62	135157.
7.60	135127.
7.54	133134.
7.40	128410.
7.43	128929.
7.48	130190.
7.21	120550.
7.24	121214.
7.25	121757.
6.94	111557.
6.94	110844.
6.92	110470.
6.65	101378.
6.65	101104.
6.63	100632.
6.29	92370.
6.30	92585.
6.35	93195.
5.99	85640.
6.04	86184.
6.05	86212.
5.52	76532.
5.50	76026.
5.49	75952.
5.00	68641.
5.00	68413.
4.96	68142.
4.47	63753.
4.50	64015.
4.48	63808.
3.87	55060.
3.83	54712.
3.84	54842.
3.27	48393.
3.18	47855.
3.17	47643.
2.59	42446.
2.54	42217.
2.52	42028.
1.93	35253.
1.96	35341.
1.97	35674.
1.34	28280.
1.31	28068.
1.32	27986.
0.79	20786.
0.75	20484.
0.72	20166.
0.40	15124.
0.37	14143.

R134a/RL68H (98/2)
File: RL682TB.dat

ΔT_s (K)	q'' (W/m^2)
6.80	131516.
6.83	133144.
6.87	135226.
6.67	128961.
6.70	129817.
6.71	130436.
6.39	120044.
6.38	119585.

6.39	119522.
6.16	110287.
6.16	109898.
6.14	109491.
5.95	101777.
5.91	100204.
5.81	96935.
5.74	93375.
5.75	93728.
5.78	94439.
5.54	85394.
5.55	85785.
5.57	86239.
5.28	76217.
5.26	75926.
5.25	75900.
4.95	69652.
4.91	68631.
4.92	68771.
4.21	58611.
4.30	60076.
4.37	60779.
3.84	52392.
3.82	52289.
3.82	52070.
3.19	45529.
3.09	44931.
3.09	43891.
2.47	37490.
2.42	37239.
2.41	37085.
1.95	31667.
1.86	30822.
1.85	30881.
1.28	23924.
1.19	23135.
1.17	23104.
0.73	17744.
0.67	17225.
0.66	17184.
0.28	11605.
7.15	135184.
7.15	135544.
7.19	136499.
6.92	128301.
6.92	128034.
6.92	128106.
6.61	118215.
6.62	118295.
6.61	117478.
6.42	111059.
6.40	109973.
6.39	109599.
6.16	100919.
6.16	100786.
6.18	100732.
5.95	93297.
5.94	92678.
5.93	92342.
5.70	83802.
5.70	83589.
5.74	84325.
5.45	75820.
5.46	75996.
5.48	76058.

5.05	67516.
4.98	66639.
4.99	66739.
4.42	57243.
4.43	57208.
4.39	57251.
3.79	50104.
3.80	50467.
3.80	50496.
3.12	44448.
3.13	44891.
3.17	45198.
2.48	37336.
2.49	37647.
2.51	37877.
1.92	31266.
1.86	31004.
1.85	30947.
1.33	24756.
1.30	24552.
1.30	24622.
0.70	17501.
0.63	16846.
0.60	16730.
0.29	11557.
7.07	139285.
7.12	140126.
7.14	140076.
6.91	132120.
6.91	131552.
6.93	131381.
6.71	123959.
6.71	123989.
6.72	123857.
6.53	114209.
6.52	113595.
6.59	115651.
6.34	106034.
6.32	105069.
6.32	104844.
6.10	95342.
6.10	94925.
6.10	94520.
5.92	85929.
5.89	85412.
5.93	86035.
5.64	76937.
5.69	78339.
5.70	78388.
5.35	71796.
5.33	69122.
5.31	68529.
4.88	64061.
4.87	62127.
4.87	62190.
4.22	54429.
4.14	53460.
4.18	53996.
3.70	48747.
3.74	49458.
3.81	49885.
2.96	42665.
2.98	42848.
2.95	42572.
2.29	35227.

2.25	34972.
2.22	34605.
1.76	29183.
1.68	28589.
1.68	28444.
1.12	22021.
1.06	21356.
1.06	21331.
0.55	14315.
6.85	136105.
6.85	136232.
6.84	136217.
6.62	128082.
6.60	127638.
6.59	127458.
6.37	119260.
6.35	118798.
6.35	118655.
6.15	110567.
6.11	109686.
6.11	109194.
5.89	100525.
5.85	98582.
5.82	97622.
5.67	91219.
5.69	91961.
5.71	92450.
5.38	81174.
5.39	81098.
5.40	81354.
5.09	72304.
5.08	72056.
5.05	71648.
4.61	64809.
4.60	64782.
4.60	64755.
4.05	58971.
3.95	58312.
3.98	58846.
3.51	51349.
3.46	52563.
3.52	51740.
2.91	44665.
2.85	44401.
2.84	44312.
2.23	38477.
2.16	37804.
2.11	37374.
1.57	31101.
1.48	30443.
1.48	30402.
0.96	23374.
0.99	24180.
1.03	24607.
0.42	16590.
0.41	16552.
0.41	16212.
6.65	127961.
6.67	129033.
6.71	130411.
6.50	123555.
6.48	123497.
6.50	124244.
6.27	115587.
6.26	115813.

6.28	116209.
6.05	107922.
6.08	108020.
6.08	108402.
5.77	96858.
5.76	96656.
5.76	96374.
5.57	89966.
5.57	87670.
5.56	87682.
5.29	77633.
5.28	76929.
5.28	77065.
4.99	69800.
4.96	69233.
4.92	68370.
4.53	61548.
4.39	60298.
4.43	60546.
3.82	55154.
3.80	55037.
3.77	54850.
3.27	47303.
3.24	47255.
3.29	47859.
2.67	42136.
2.66	42067.
2.65	42259.
2.01	34682.
1.93	33982.
1.88	33749.
1.40	28034.
1.39	28195.
1.42	28356.
0.81	20784.
0.78	20614.
0.76	20414.
0.37	14572.
0.31	14175.
6.76	137233.
6.78	136837.
6.77	136684.
6.51	128307.
6.50	127860.
6.50	127582.
6.26	119647.
6.17	117044.
6.17	116773.
6.03	112290.
6.01	112358.
6.03	112694.
5.76	102098.
5.75	102445.
5.77	102941.
5.55	93328.
5.53	92932.
5.52	92886.
5.30	85430.
5.24	83062.
5.27	85521.
4.94	73658.
4.95	73365.
4.97	73840.
4.61	66293.
4.53	65038.

4.53	64816.
3.97	56957.
3.94	58802.
3.93	56910.
3.41	52081.
3.39	50746.
3.37	50627.
2.85	44485.
2.81	44302.
2.78	43881.
2.16	37602.
2.20	38001.
2.15	37798.
1.61	31275.
1.60	30966.
1.54	30443.
1.06	24331.
0.97	23546.
0.92	22746.
0.56	17961.
0.52	17590.
0.51	17494.
0.16	12175.
6.79	136466.
6.81	136451.
6.79	136327.
6.57	128235.
6.54	127634.
6.53	127436.
6.30	119108.
6.28	118564.
6.28	118361.
6.07	110582.
6.06	109692.
6.03	109384.
5.80	100806.
5.79	100020.
5.77	99194.
5.59	92047.
5.62	92660.
5.64	93875.
5.35	84016.
5.39	84456.
5.40	84997.
5.04	73728.
5.04	73376.
5.02	72932.
4.62	65128.
4.55	64321.
4.55	63975.
4.05	57107.
4.01	59076.
3.99	58653.
3.38	51260.
3.38	51255.
3.40	50181.
2.88	44164.
2.89	44333.
2.90	44596.
2.22	37349.
2.17	37174.
2.16	37138.
1.64	31082.
1.61	30979.
1.59	30936.
1.11	24623.
1.04	24167.
1.03	24038.
0.54	17248.
0.49	16790.
0.46	16467.
0.20	12753.
0.18	12480.

R134a/RL681Al0 (99.5/0.5)
File: TBAl5.dat

ΔT_s (K)	q'' (W/m^2)
8.10	126996.
8.09	127082.
8.05	127186.
7.73	119787.
7.75	119840.
7.73	119787.
7.35	110818.
7.29	109826.
7.32	110051.
7.01	103563.
7.02	103543.
7.08	104321.
6.62	95512.
6.64	95378.
6.65	95462.
6.18	86315.
6.17	86062.
6.14	85821.
5.76	79334.
5.66	77576.
5.59	76606.
5.30	72227.
5.33	74810.
5.39	75544.
4.76	64135.
4.74	63977.
4.74	63717.
4.23	56893.
4.22	56854.
4.23	56916.
3.62	49391.
3.61	49408.
3.51	48179.
3.01	43642.
3.04	44015.
3.07	44406.
2.45	37329.
2.33	36872.
2.35	36857.
1.75	30647.
1.68	30274.
1.68	30021.
1.04	23117.
0.99	22829.
0.98	22574.
0.51	17181.
0.48	16883.
7.91	124009.
7.87	122943.
7.81	122027.
7.44	114447.
7.44	114684.
7.49	115392.
7.14	107938.
7.17	108317.
7.23	109166.
6.75	99806.
6.77	100079.
6.81	100321.
6.40	92532.
6.39	92265.
6.41	92295.
5.91	83693.
5.95	83860.
5.90	83277.
5.45	75933.
5.41	75567.
5.44	75498.
5.05	71987.
5.00	71281.
4.96	70806.
4.52	61831.
4.55	62203.
4.60	62579.
3.96	54391.
3.90	53920.
3.91	54085.
3.39	48026.
3.42	48098.
3.39	47987.
2.80	42662.
2.74	42148.
2.74	42081.
2.04	34675.
2.02	34546.
2.01	34267.
1.42	27915.
1.32	26619.
1.31	26439.
0.76	20444.
0.76	20362.
0.76	20272.
0.42	15745.
0.37	15331.
7.94	128952.
7.92	128990.
7.89	128226.
7.49	119673.
7.45	119441.
7.53	120481.
7.19	112722.
7.22	113208.
7.25	113430.
6.79	104301.
6.76	103731.
6.77	103733.
6.46	96554.
6.45	96280.
6.43	95996.
6.04	88222.
6.11	89036.
5.99	86976.
5.59	80352.
5.55	79301.
5.52	78996.

5.13	72788.
5.14	73248.
5.13	72695.
4.70	66423.
4.60	65254.
4.64	65692.
4.10	58096.
4.13	58611.
4.18	58803.
3.48	50652.
3.48	50729.
3.46	50553.
2.94	45684.
2.87	44981.
2.87	44928.
2.28	38245.
2.14	37129.
2.14	36833.
1.59	30453.
1.52	29919.
1.52	29998.
0.90	23229.
0.91	23161.
0.90	22999.
0.50	17860.
0.47	17163.
0.46	16977.
0.22	13606.
7.65	122507.
7.61	122208.
7.57	121902.
7.21	114448.
7.18	113850.
7.18	112328.
6.81	105160.
6.83	105505.
6.88	106156.
6.42	97675.
6.47	97937.
6.48	98363.
6.02	89736.
6.00	89075.
6.00	88634.
5.56	80738.
5.53	80298.
5.52	79883.
5.08	72599.
5.05	72007.
5.07	72020.
4.65	65404.
4.58	64723.
4.62	65377.
4.16	61300.
4.17	59356.
4.25	60236.
3.53	51192.
3.45	50585.
3.45	50336.
2.89	43705.
2.83	44735.
2.85	43514.
2.20	37750.
2.20	37582.
2.22	37878.
1.57	30735.

1.49	29970.
1.43	29407.
1.01	24451.
1.01	24522.
1.03	24808.
0.61	19074.
0.56	18672.
0.55	18451.
0.17	12540.
7.50	123212.
7.51	123523.
7.51	123835.
7.21	117157.
7.23	117368.
7.27	118298.
6.81	108674.
6.80	108779.
6.80	108869.
6.44	101596.
6.45	101534.
6.45	101206.
6.08	93778.
6.03	92969.
5.99	92411.
5.53	83981.
5.52	83559.
5.51	83360.
5.18	77441.
5.09	75956.
5.08	75633.
4.73	70505.
4.74	70714.
4.78	71243.
4.18	62805.
4.20	62828.
4.24	63031.
3.58	54826.
3.53	54332.
3.54	54531.
2.92	46983.
2.89	48041.
2.89	48005.
2.30	41079.
2.28	41315.
2.29	40925.
1.78	34763.
1.71	34135.
1.68	33775.
1.21	28237.
1.19	28262.
1.21	28531.
0.69	21305.
0.67	20826.
0.69	20847.
0.38	16450.
0.35	16142.
7.51	124215.
7.41	122149.
7.35	121562.
7.08	115556.
7.11	116193.
7.17	117266.
6.81	109977.
6.83	110490.
6.86	110937.

6.48	103147.
6.44	102178.
6.42	101822.
6.00	93614.
5.99	93193.
5.98	92930.
5.59	86151.
5.44	83200.
5.36	82137.
5.15	77817.
5.20	78357.
5.24	78817.
4.74	70818.
4.77	71231.
4.78	71434.
4.22	63183.
4.17	64977.
4.19	63188.
3.65	55551.
3.60	55159.
3.67	55780.
2.97	47770.
2.86	48006.
3.10	48662.
2.55	43496.
2.52	43423.
2.50	43153.
1.87	36198.
1.83	35826.
1.88	36459.
1.31	29289.
1.30	28900.
1.28	28694.
0.65	21113.
0.66	21242.
0.68	21504.
0.29	15479.
0.27	15159.
7.34	121504.
7.37	122157.
7.41	122896.
7.09	115680.
7.08	115664.
7.08	115892.
6.69	107523.
6.69	107640.
6.71	107728.
6.37	100262.
6.36	99957.
6.34	99487.
5.94	91441.
5.95	91828.
5.97	91698.
5.56	84476.
5.56	84462.
5.61	85138.
5.14	76893.
5.09	76076.
5.14	76719.
4.60	68718.
4.61	68481.
4.61	68423.
4.13	62116.
4.07	63856.
4.09	63908.

3.62	55525.
3.59	54987.
3.56	54710.
3.01	47945.
3.02	47905.
3.06	48661.
2.38	42136.
2.38	42193.
2.38	42284.
1.82	35323.
1.81	35240.
1.78	35087.
1.30	28972.
1.23	28374.
1.20	28106.
0.66	20966.
0.61	20567.
0.61	20329.
0.31	15904.
0.28	15584.
0.27	15240.

R134a/RL681Al0 (99/1)
File: TBAl1.dat

ΔT_s (K)	q'' (W/m^2)
7.95	132140.
7.92	132013.
7.84	129425.
7.69	125312.
7.72	126020.
7.77	127297.
7.42	117269.
7.43	117232.
7.42	117004.
7.17	108695.
7.14	107954.
7.16	106655.
6.84	98089.
6.75	95369.
6.66	93311.
6.53	90206.
6.60	90777.
6.65	91359.
6.17	81125.
6.15	80757.
6.14	80807.
5.74	75086.
5.74	73772.
5.72	74723.
5.22	66470.
5.15	65710.
5.20	65115.
4.74	59280.
4.78	60020.
4.81	59021.
4.07	50952.
4.07	50956.
4.08	51050.
3.37	43406.
3.32	43084.
3.30	43056.
2.63	36035.
2.58	35650.
2.55	35421.
1.96	29404.
1.87	28887.
1.89	29011.
1.30	22951.
1.25	22691.
1.25	22660.
0.73	17314.
0.69	16984.
0.68	16842.
0.25	11957.
7.77	129838.
7.80	131230.
7.84	132294.
7.62	125614.
7.64	125982.
7.65	126030.
7.35	117328.
7.34	116664.
7.33	116258.
7.10	107396.
7.09	106953.
7.05	105534.
6.78	97778.
6.82	98275.
6.86	99078.
6.48	90369.
6.52	90809.
6.54	91088.
6.02	80801.
6.05	80862.
6.03	80455.
5.61	73270.
5.57	72664.
5.57	72237.
5.09	64390.
5.01	65227.
5.03	65540.
4.64	57955.
4.67	58189.
4.69	58541.
3.97	50801.
3.93	50674.
3.93	50699.
3.39	44754.
3.33	44399.
3.32	44376.
2.64	36830.
2.53	36139.
2.51	35754.
1.90	29607.
1.84	29371.
1.86	29236.
1.36	24132.
1.33	23963.
1.32	23930.
0.75	18000.
0.72	17620.
0.72	17513.
0.34	13131.
7.74	128216.
7.76	129120.
7.79	130178.
7.49	121910.
7.49	121837.
7.51	122209.
7.21	113673.
7.21	113477.
7.23	113332.
6.96	104105.
6.95	103564.
6.95	103081.
6.58	93222.
6.57	92867.
6.57	92520.
6.29	86171.
6.15	83691.
6.03	83249.
5.91	79156.
5.93	79781.
5.90	79112.
5.34	71120.
5.38	70251.
5.37	71622.
4.86	62120.
4.82	61655.
4.80	62329.
4.15	54016.
4.12	53786.
4.12	53711.
3.63	48155.
3.62	47913.
3.59	47767.
2.94	40687.
2.89	40554.
2.93	40882.
2.28	34394.
2.29	34466.
2.30	34649.
1.55	26942.
1.52	26714.
1.50	26564.
0.97	20797.
0.92	20483.
0.92	20440.
0.52	15625.
0.48	14909.
0.44	14647.
7.74	127021.
7.78	128300.
7.82	128350.
7.54	120601.
7.56	122102.
7.58	122704.
7.24	111584.
7.25	111317.
7.27	111079.
6.99	102335.
6.99	101525.
6.97	100996.
6.59	92537.
6.60	92377.
6.59	91402.
6.30	84771.
6.31	84645.
6.32	84863.
5.80	76082.
5.82	76096.

5.80	75849.
5.46	70298.
5.46	70207.
5.42	69750.
4.89	61664.
4.87	61056.
4.70	58793.
4.32	53966.
4.35	54719.
4.37	54884.
3.56	45908.
3.56	45972.
3.56	45845.
3.00	41443.
2.94	41144.
2.94	41098.
2.26	34204.
2.20	33758.
2.19	33661.
1.62	27862.
1.52	27006.
1.50	26931.
0.97	21308.
0.94	21134.
0.95	21032.
0.53	15999.
0.49	15455.
0.46	15203.
0.19	11468.
7.62	127901.
7.60	127972.
7.66	129487.
7.41	120707.
7.42	121121.
7.42	121086.
7.11	112292.
7.10	111343.
7.12	111052.
6.89	103846.
6.85	102303.
6.74	99670.
6.52	92727.
6.57	93452.
6.61	94409.
6.22	85708.
6.22	85684.
6.23	85842.
5.78	77079.
5.75	76590.
5.75	76655.
5.35	69826.
5.36	69903.
5.36	69753.
4.72	59710.
4.61	58647.
4.60	58409.
4.26	53791.
4.27	54306.
4.34	54962.
3.63	48560.
3.61	48235.
3.60	48105.
2.97	41327.
2.91	40916.
2.88	40566.

2.23	34365.
2.21	34116.
2.15	33103.
1.61	27811.
1.53	27252.
1.50	27086.
0.89	20493.
0.88	20318.
0.88	20392.
0.42	14654.
0.38	14192.
7.55	129631.
7.47	128021.
7.50	129134.
7.26	122315.
7.27	122575.
7.29	123495.
7.03	113562.
7.03	113017.
7.02	112626.
6.77	103451.
6.76	103259.
6.73	102657.
6.44	94776.
6.45	94861.
6.49	95575.
6.11	87178.
6.12	87408.
6.17	88141.
5.68	79064.
5.67	78867.
5.66	78717.
5.29	72152.
5.31	72034.
5.30	72176.
4.65	63545.
4.62	61588.
4.50	59727.
4.12	56254.
4.12	56475.
4.16	57151.
3.58	50097.
3.56	49835.
3.58	50064.
2.79	41630.
2.75	41215.
2.74	40889.
2.00	33119.
2.02	33725.
2.06	33773.
1.53	28126.
1.42	27332.
1.40	27129.
0.91	21503.
0.86	21256.
0.87	21236.
0.45	15564.
0.40	14867.
7.89	132854.
7.86	131401.
7.82	131522.
7.49	121285.
7.52	121984.
7.55	122674.
7.19	112680.

7.23	113201.
7.25	113622.
6.95	104604.
6.95	104135.
6.97	104299.
6.65	94756.
6.64	94639.
6.68	95521.
6.19	84108.
6.10	83016.
6.12	83277.
5.78	77136.
5.80	77602.
5.85	78408.
5.27	67534.
5.24	67265.
5.23	67299.
4.66	59757.
4.64	59473.
4.61	58981.
3.99	52790.
3.95	52616.
3.97	52697.
3.33	45813.
3.33	45842.
3.31	45704.
2.68	39303.
2.63	38973.
2.63	39060.
1.87	31173.
1.81	30844.
1.81	30956.
1.11	23316.
1.09	23240.
1.08	23082.
0.62	17699.
0.61	17353.
0.59	17194.
0.20	12188.
0.17	11941.
0.15	11721.

R134a/RL681Al0 (98/2)
File: TBAl2.dat

ΔT_s (K)	q'' (W/m^2)
7.47	140536.
7.45	140202.
7.41	139402.
7.22	132786.
7.25	133667.
7.25	133327.
6.96	125184.
6.99	126469.
6.97	126268.
6.64	116601.
6.65	117350.
6.67	117945.
6.41	108955.
6.43	109174.
6.46	109249.
6.24	100418.
6.26	99748.

6.32	99351.
6.06	90414.
6.10	90487.
6.13	89911.
5.83	81223.
5.84	80963.
5.88	81224.
5.43	71201.
5.44	70982.
5.47	70971.
5.12	64420.
5.13	64409.
5.10	62301.
4.60	55182.
4.57	55151.
4.53	56266.
3.96	49710.
3.90	49409.
3.88	49276.
3.28	42845.
3.21	42352.
3.20	42171.
2.51	35293.
2.50	35382.
2.53	35656.
1.97	29936.
1.86	28944.
1.83	28714.
1.15	21687.
1.11	21355.
1.10	21267.
0.47	14417.
7.31	137044.
7.29	136833.
7.25	136400.
7.02	127619.
6.99	126553.
7.03	128451.
6.76	119755.
6.77	121224.
6.76	120657.
6.51	113582.
6.51	113432.
6.51	114423.
6.19	105224.
6.26	105371.
6.29	105173.
6.09	94747.
6.12	94331.
6.16	94627.
5.94	85014.
5.93	83983.
5.82	80722.
5.64	76217.
5.66	76143.
5.69	76216.
5.27	68029.
5.29	68140.
5.33	68540.
4.82	59177.
4.81	58979.
4.77	58656.
4.12	52818.
4.10	52484.
4.06	52349.

3.52	46769.
3.43	45870.
3.36	45255.
2.81	39533.
2.79	39535.
2.85	39976.
2.13	33033.
2.13	33030.
2.13	33067.
1.51	26678.
1.41	25846.
1.37	25286.
0.82	19652.
7.44	129204.
7.60	136664.
7.63	138102.
7.40	133374.
7.42	131786.
7.47	132870.
7.18	125004.
7.19	125762.
7.21	126155.
6.88	117705.
6.79	117416.
6.78	117155.
6.45	108533.
6.48	108324.
6.52	106734.
6.25	96124.
6.37	97878.
6.41	98224.
6.19	91483.
6.28	92324.
6.36	93787.
5.98	81655.
6.00	81616.
6.01	81310.
5.59	72947.
5.57	72366.
5.58	71963.
5.11	64080.
5.07	63687.
5.08	63911.
4.57	56665.
4.57	56568.
4.56	56359.
4.04	50095.
4.04	50871.
4.28	53083.
3.16	41828.
3.05	40734.
2.93	39357.
2.58	35840.
2.32	33652.
2.23	32815.
1.55	25901.
1.38	24467.
7.19	139135.
7.19	138825.
7.12	138808.
6.95	130712.
6.94	130480.
6.88	130454.
6.74	122978.
6.65	122553.

6.66	122124.
6.42	114044.
6.41	113262.
6.46	112374.
6.26	104989.
6.33	105314.
6.42	105488.
6.08	95225.
6.10	94894.
6.15	94528.
5.95	87383.
5.99	87305.
6.00	86888.
5.71	77650.
5.85	79821.
5.88	80355.
5.08	66423.
5.13	66525.
5.08	65739.
4.70	60259.
4.67	60106.
4.53	60259.
3.96	52551.
3.98	52515.
3.50	47733.
3.49	47780.
7.37	138827.
7.33	138743.
7.31	138896.
6.99	130378.
6.98	130418.
6.97	130325.
6.67	122204.
6.76	122463.
6.73	122641.
6.43	113347.
6.41	113378.
6.43	113408.
6.20	105201.
6.23	105023.
6.28	104861.
5.99	94502.
6.04	94347.
6.06	93962.
5.80	84381.
5.81	83761.
5.81	83337.
5.62	77453.
5.61	76896.
5.56	75680.
5.21	67980.
5.26	68351.
5.28	68822.
4.72	60023.
4.76	60328.
4.79	59414.
4.29	54279.
4.26	54048.
4.25	53806.
3.55	46148.
3.51	45886.
3.49	45548.
2.91	39818.
2.89	39654.
2.90	39572.

2.22	32527.
2.09	32163.
2.09	31880.
1.66	26836.
1.62	26629.
1.61	26521.
1.07	20772.
1.00	20220.
7.38	136027.
7.39	136359.
7.42	137368.
7.10	128435.
7.08	128582.
7.08	128810.
6.80	121044.
6.76	120721.
6.74	120598.
6.50	112841.
6.51	112452.
6.53	112211.

6.31	103990.
6.34	103555.
6.38	103216.
6.16	95587.
6.19	94761.
6.23	94223.
5.95	83947.
5.96	83327.
6.02	83945.
5.74	77109.
5.78	77243.
5.80	77538.
5.34	68783.
5.34	68372.
5.33	68072.
4.75	59565.
4.73	59188.
4.72	57793.
4.21	52962.
4.19	52905.

4.20	52832.
3.68	47465.
3.64	46914.
3.62	46650.
2.85	38800.
2.81	38610.
2.81	38656.
2.27	32831.
2.21	32459.
2.21	32373.
1.60	26519.
1.64	26885.
1.66	27001.
0.82	17703.
0.75	17193.
0.71	16840.
0.29	11982.
0.20	11714.

Table 3 Number of test days and data points

Fluid (% mass fraction)	Number of days	Number of data points
Pure R134a 0.1 K ≤ ΔT_s ≤ 6.3 K	6	250
R134a/RL68H (99.5/0.5) 0.12 K ≤ ΔT_s ≤ 7.6 K	7	320
R134a/RL68H (99/1) 0.1 K ≤ ΔT_s ≤ 7.6 K	6	282
R134a/RL68H (98/2) 0.1 K ≤ ΔT_s ≤ 7.1 K	7	337
R134a/RL681AlO (99.5/0.5) 0.17 K ≤ ΔT_s ≤ 7.8 K	7	325
R134a/RL681AlO (99/1) 0.18 K ≤ ΔT_s ≤ 7.8 K	7	330
R134a/RL681AlO (98/2) 0.12 K ≤ ΔT_s ≤ 7.1 K	6	264

Table 4 Estimated parameters for cubic boiling curve fits for Turbo-BII-HP copper surface

$\Delta T_s = A_0 + A_1\, q" + A_2\, q"^2 + A_3\, q"^3$

ΔT_s in kelvin and $q"$ in W/m^2

Fluid	A_o	A_1	A_2	A_3
Pure R134a 0.1 K ≤ ΔT_s ≤ 6.3 K	-0.740527	4.95277 x10^{-5}	2.63884 x10^{-10}	- 1.81569x10^{-15}
R134a/RL68H (99.5/0.5) 0.12 K ≤ ΔT_s ≤ 3.8 K 3.8 K ≤ ΔT_s ≤ 7.6 K	0.252376 -3.29612	-4.07073x10^{-5} 1.64852 x10^{-4}	2.76832 x10^{-9} -1.00471x10^{-9}	-1.99733 x10^{-14} 2.90580 x10^{-15}
R134a/RL68H (99/1) 0.1 K ≤ ΔT_s ≤ 4.0 K 4.0 K ≤ ΔT_s ≤ 7.6 K	-0.051371 -6.60753	5.16322 x10^{-6} 2.89968x10^{-4}	1.90984 x10^{-9} -2.24421x10^{-9}	-1.39618 x10^{-14} 6.50065x10^{-15}
R134a/RL68H (98/2) 0.1 K ≤ ΔT_s ≤ 5.0 K 5.0 K ≤ ΔT_s ≤ 7.1 K	-0.243947 0.580891	1.95563x10^{-5} 1.10818x10^{-4}	1.91732 x10^{-9} -8.53909x10^{-10}	-1.61984x10^{-14} 2.80652x10^{-15}
R134a/RL681AlO (99.5/0.5) 0.17 K ≤ ΔT_s ≤ 3.3 K 3.3 K ≤ ΔT_s ≤ 7.8 K	-0.123590 -1.58427	-9.70313x10^{-6} 1.24654x10^{-4}	3.00869x10^{-9} -5.43675x10^{-10}	-2.98665x10^{-14} 1.11426x10^{-15}
R134a/RL681AlO (99/1) 0.18 K ≤ ΔT_s ≤ 3.7 K 3.7 K ≤ ΔT_s ≤ 7.8 K	-0.516802 -3.88192	4.44071x10^{-5} 2.23548x10^{-4}	1.55037x10^{-9} -1.61582x10^{-9}	-1.40552x10^{-14} 4.49216x10^{-15}
R134a/RL681AlO (99/2) 0.12 K ≤ ΔT_s ≤ 4.4 K 4.4 K ≤ ΔT_s ≤ 7.1 K	-0.482096 -5.42332	4.94608x10^{-5} 3.05743x10^{-4}	1.43488x10^{-9} - 2.80148x10^{-9}	-1.34728x10^{-14} 9.14222x10^{-15}

Table 5 Residual standard deviation of ΔT_s

Fluid	(K)
Pure R134a	
0.1 K ≤ ΔT_s ≤ 6.3 K	0.18
R134a/RL68H (99.5/0.5)	
0.12 K ≤ ΔT_s ≤ 3.8 K	0.16
3.8 K ≤ ΔT_s ≤ 7.6 K	0.21
R134a/RL68H (99/1)	
0.1 K ≤ ΔT_s ≤ 4.0 K	0.16
4.0 K ≤ ΔT_s ≤ 7.6 K	0.18
R134a/RL68H (98/2)	
0.1 K ≤ ΔT_s ≤ 5.0 K	0.16
5.0 K ≤ ΔT_s ≤ 7.1 K	0.16
R134a/RL681AlO (99.5/0.5)	
0.17 K ≤ ΔT_s ≤ 3.3 K	0.13
3.3 K ≤ ΔT_s ≤ 7.8 K	0.19
R134a/RL681AlO (99/1)	
0.18 K ≤ ΔT_s ≤ 3.7 K	0.09
3.7 K ≤ ΔT_s ≤ 7.8 K	0.11
R134a/RL681AlO (99/2)	
0.12 K ≤ ΔT_s ≤ 4.4 K	0.07
4.4 K ≤ ΔT_s ≤ 7.1 K	0.11

Table 6 Average magnitude of 95 % multi-use confidence interval for mean $T_w - T_s$ (K)

Fluid	U (K)
Pure R134a	
0.1 K ≤ ΔT_s ≤ 6.3 K	0.07
R134a/RL68H (99.5/0.5)	
0.12 K ≤ ΔT_s ≤ 3.8 K	0.09
3.8 K ≤ ΔT_s ≤ 7.6 K	0.10
R134a/RL68H (99/1)	
0.1 K ≤ ΔT_s ≤ 4.0 K	0.10
4.0 K ≤ ΔT_s ≤ 7.6 K	0.09
R134a/RL68H (98/2)	
0.1 K ≤ ΔT_s ≤ 5.0 K	0.08
5.0 K ≤ ΔT_s ≤ 7.1 K	0.08
R134a/RL681AlO (99.5/0.5)	
0.17 K ≤ ΔT_s ≤ 3.3 K	0.08
3.3 K ≤ ΔT_s ≤ 7.8 K	0.08
R134a/RL681AlO (99/1)	
0.18 K ≤ ΔT_s ≤ 3.7 K	0.05
3.7 K ≤ ΔT_s ≤ 7.8 K	0.05
R134a/RL681AlO (99/2)	
0.12 K ≤ ΔT_s ≤ 4.4 K	0.05
4.4 K ≤ ΔT_s ≤ 7.1 K	0.05

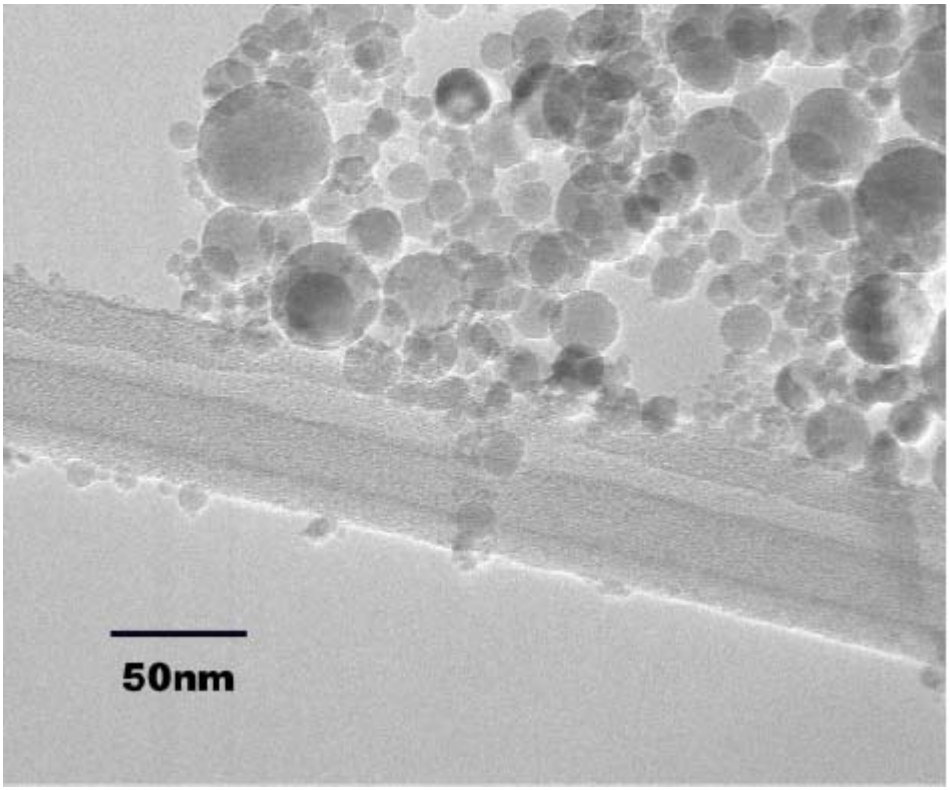

{ XE }

Fig. 1 TEM of Al_2O_3 nanolubricant (Sarkas, 2009)

{ XE **}**

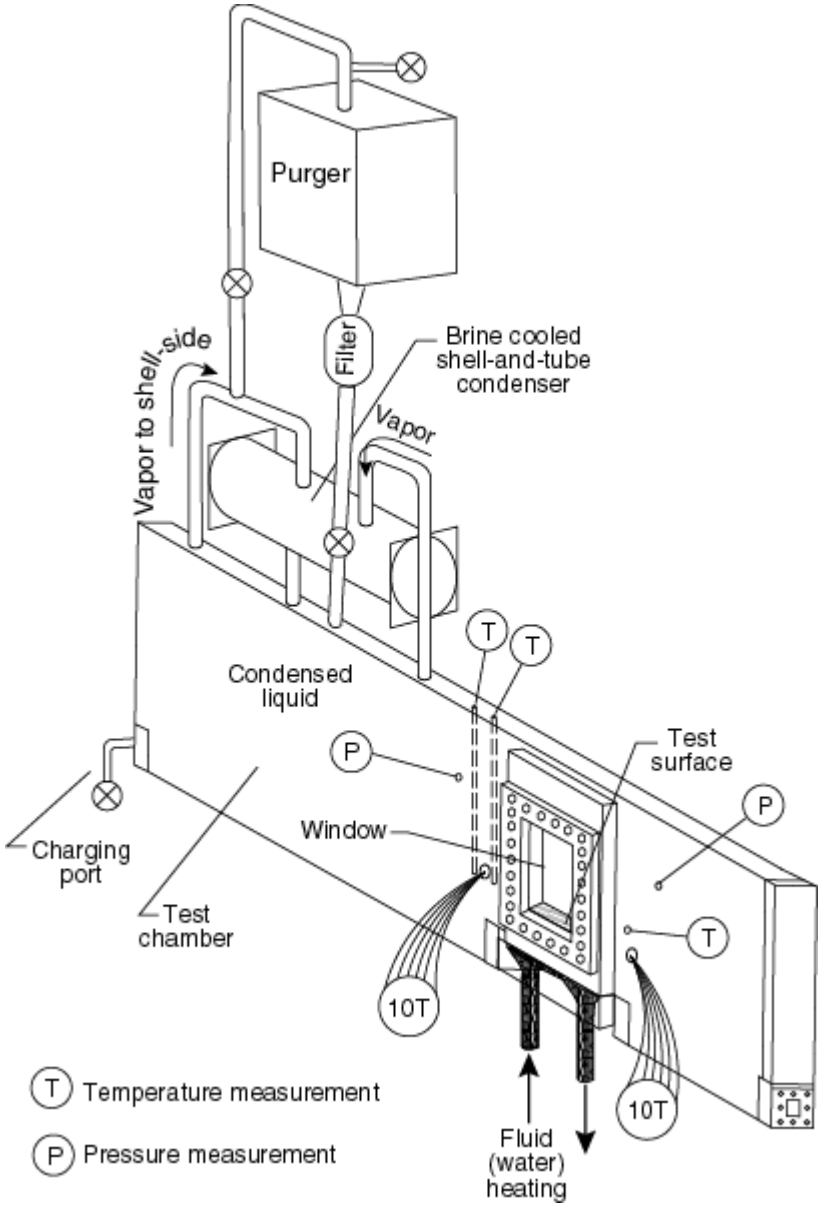

{ XE }
Fig. 2 Schematic of test apparatus

{ XE **}**

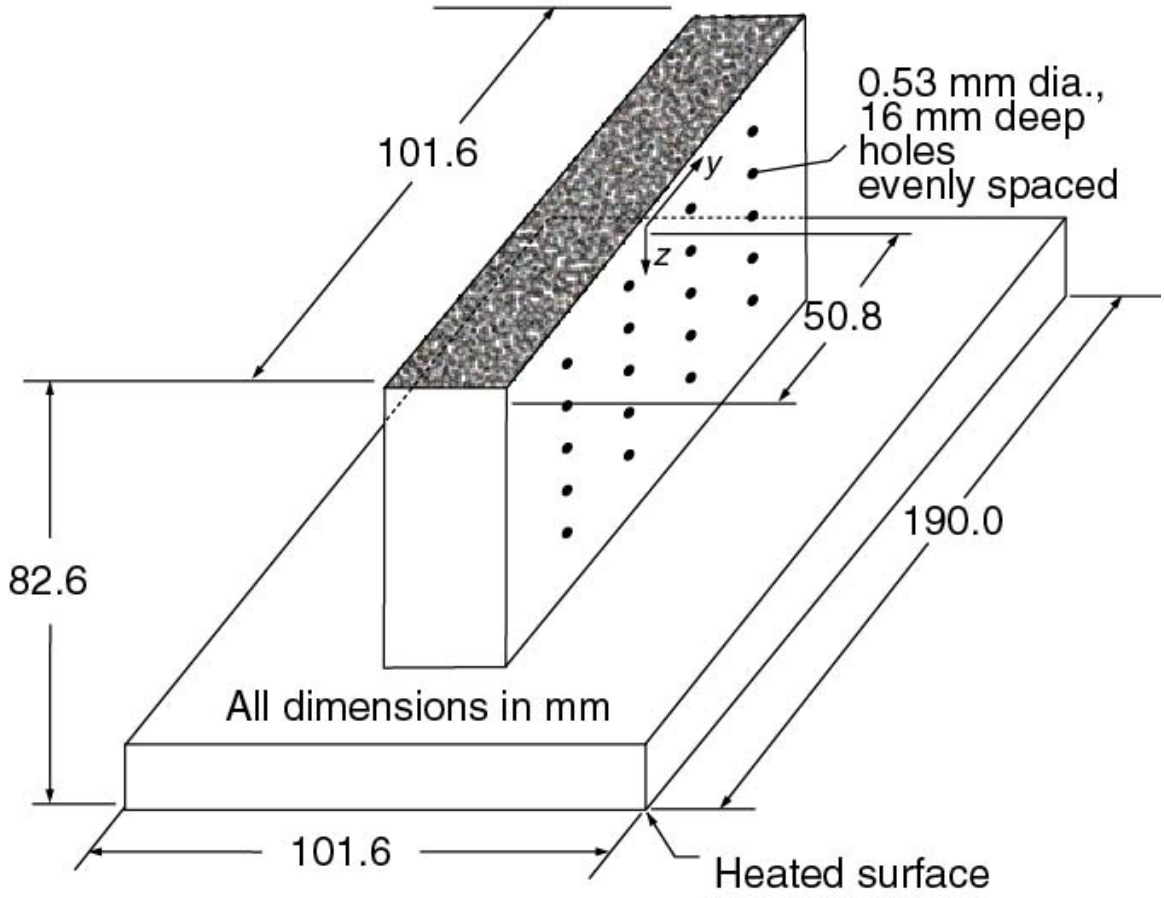

Fig. 3 OFHC copper flat test plate with Turbo-BII-HP surface and thermocouple coordinate system

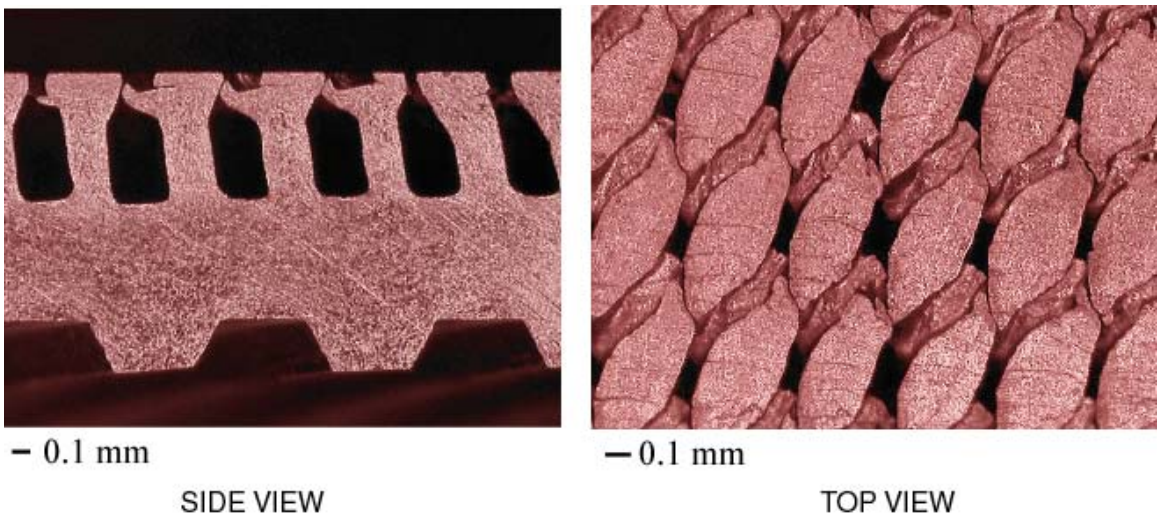

Fig. 4 Photograph of Turbo-BII-HP surface

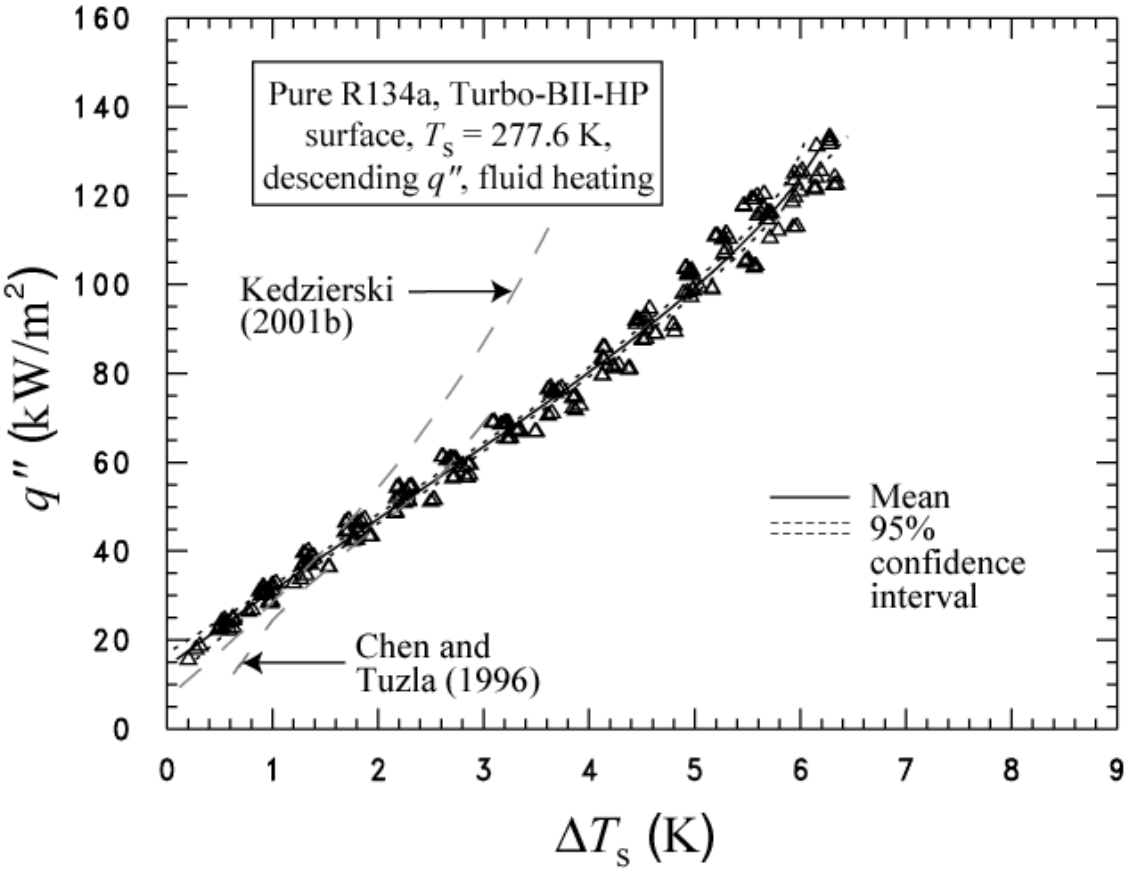

Fig. 5 Pure R134a boiling curve for Turbo-BII-HP surface

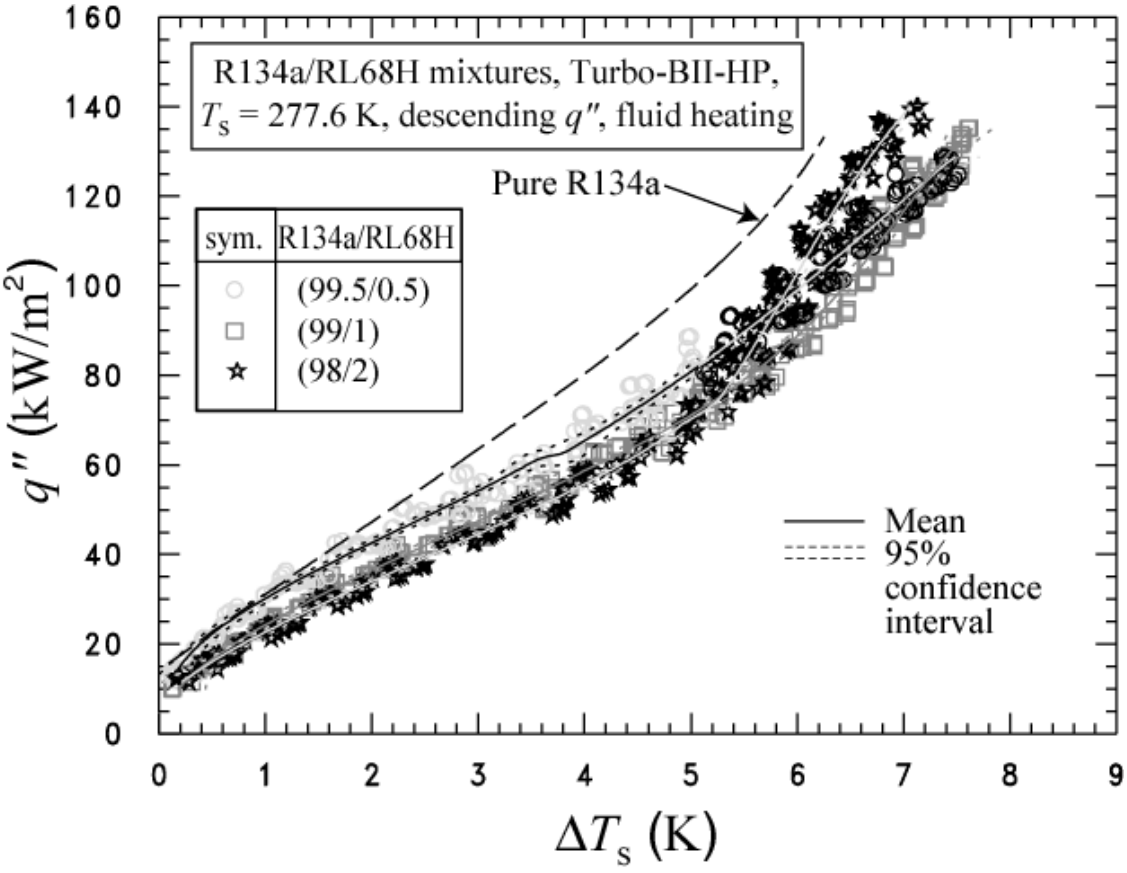

Fig. 6 R134a/RL68H mixtures boiling curves for Turbo-BII-HP surface

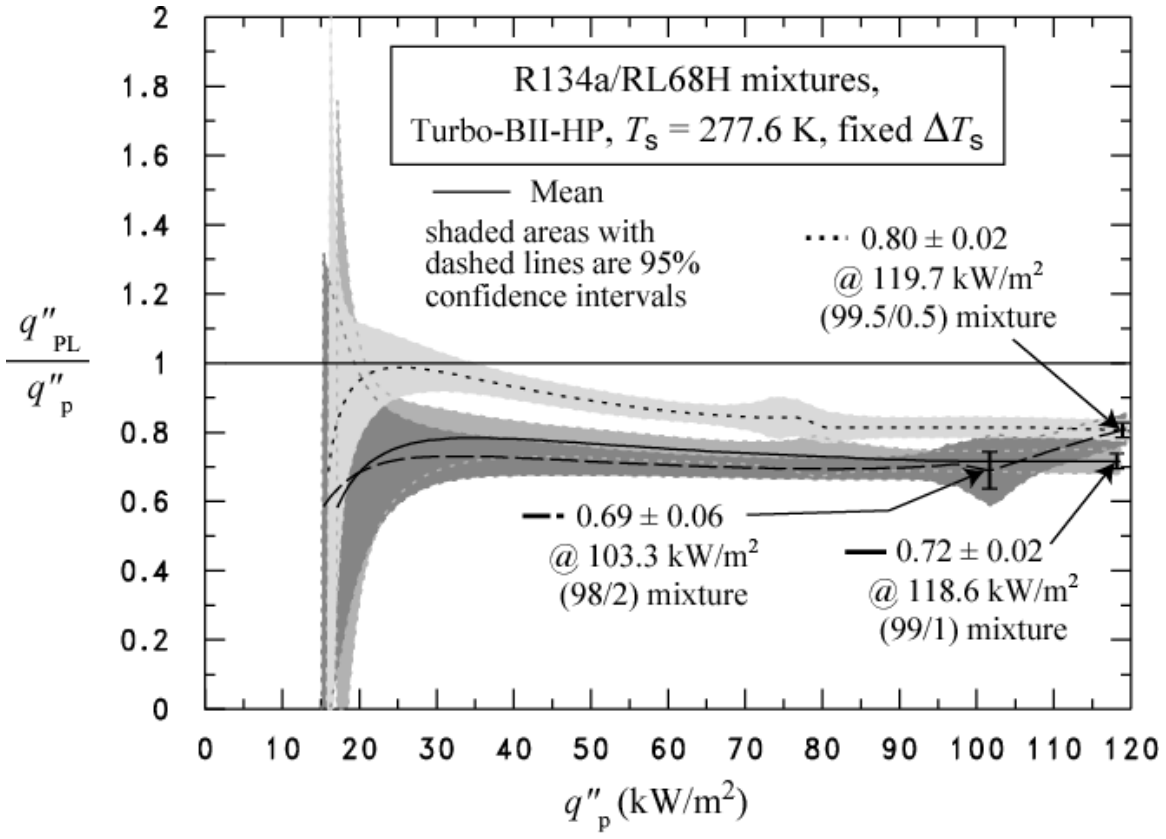

Fig. 7 Boiling heat flux of R134a/RL68H mixture relative to that of pure R134a for Turbo-BII-HP surface

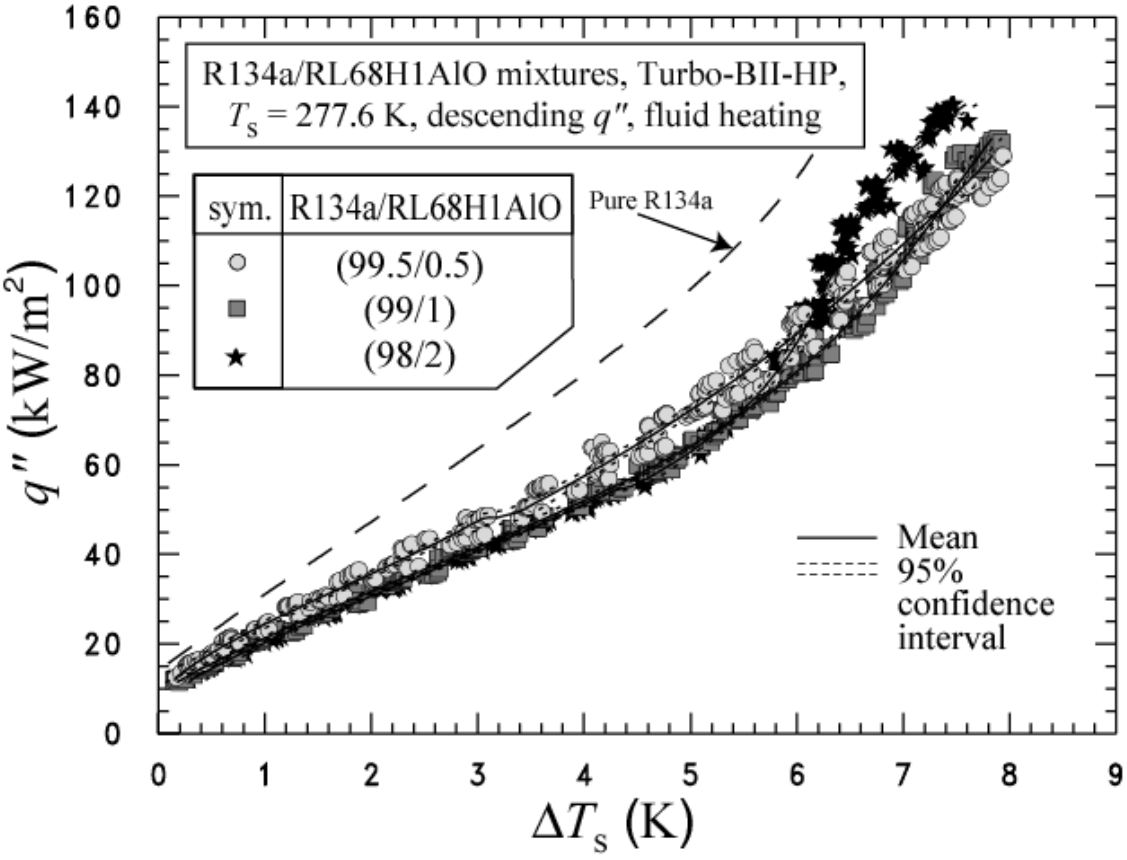

Fig. 8 R134a/RL681AlO mixtures boiling curves for Turbo-BII-HP surface

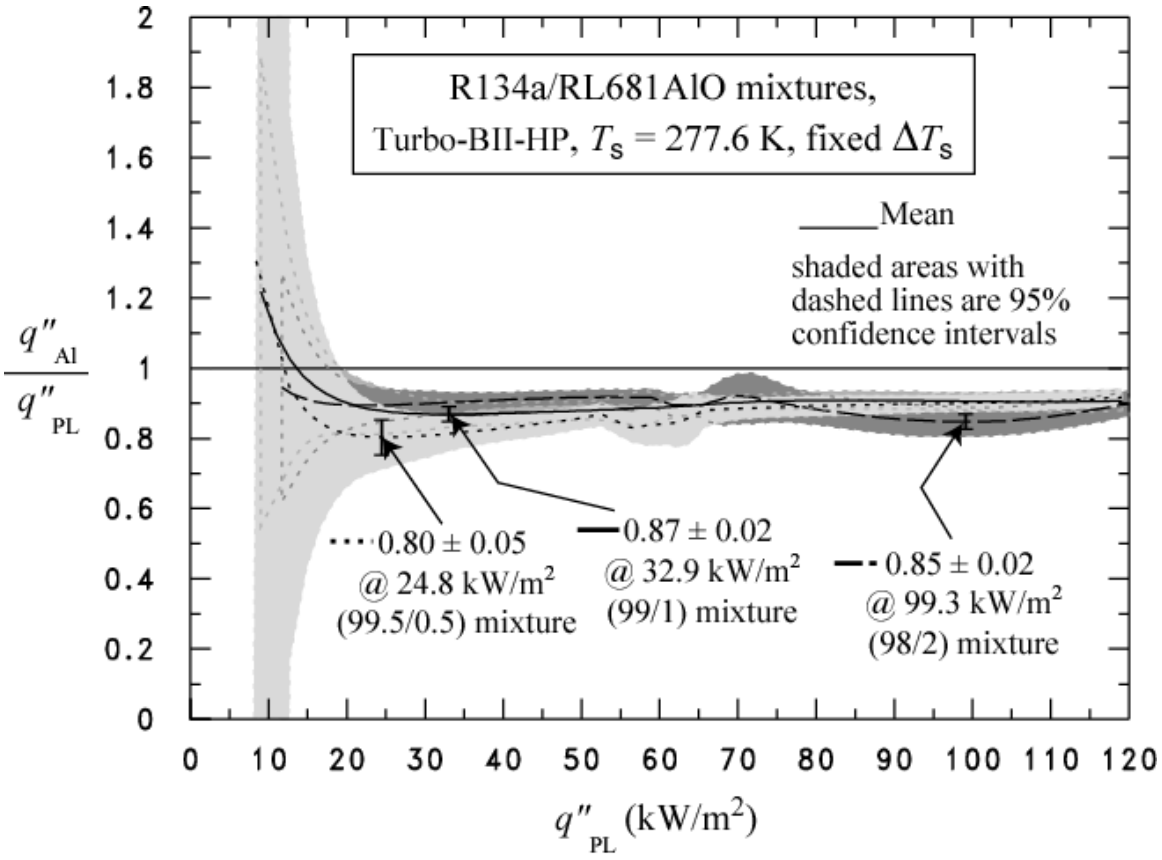

Fig. 9 Boiling heat flux of R134a/RL68H1AlO mixtures relative to that of R134a/RL68H without nanoparticles for Turbo-BII-HP surface

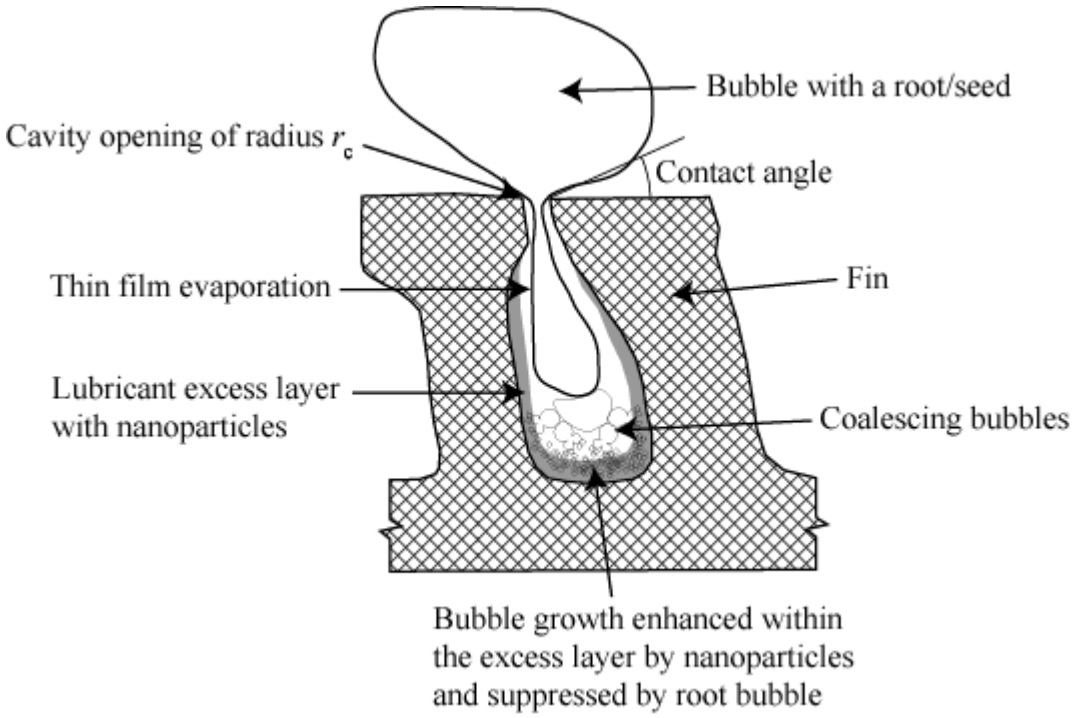

Fig. 10 Mechanistic speculation of influence of nanoparticles on reentrant cavity bubble production

APPENDIX A: UNCERTAINTIES

Figure A.1 shows the relative (percent) uncertainty of the heat flux ($U_{q"}$) as a function of the heat flux. Figure A.2 shows the uncertainty of the wall temperature as a function of the heat flux. The uncertainties shown in Figs. A.1 and A.2 are "within-run uncertainties." These do not include the uncertainties due to "between-run effects" or differences observed between tests taken on different days. The "within-run uncertainties" include only the random effects and uncertainties associated with one particular test. All other uncertainties reported in this study are "between-run uncertainties" which include all random effects such as surface past history or seeding.

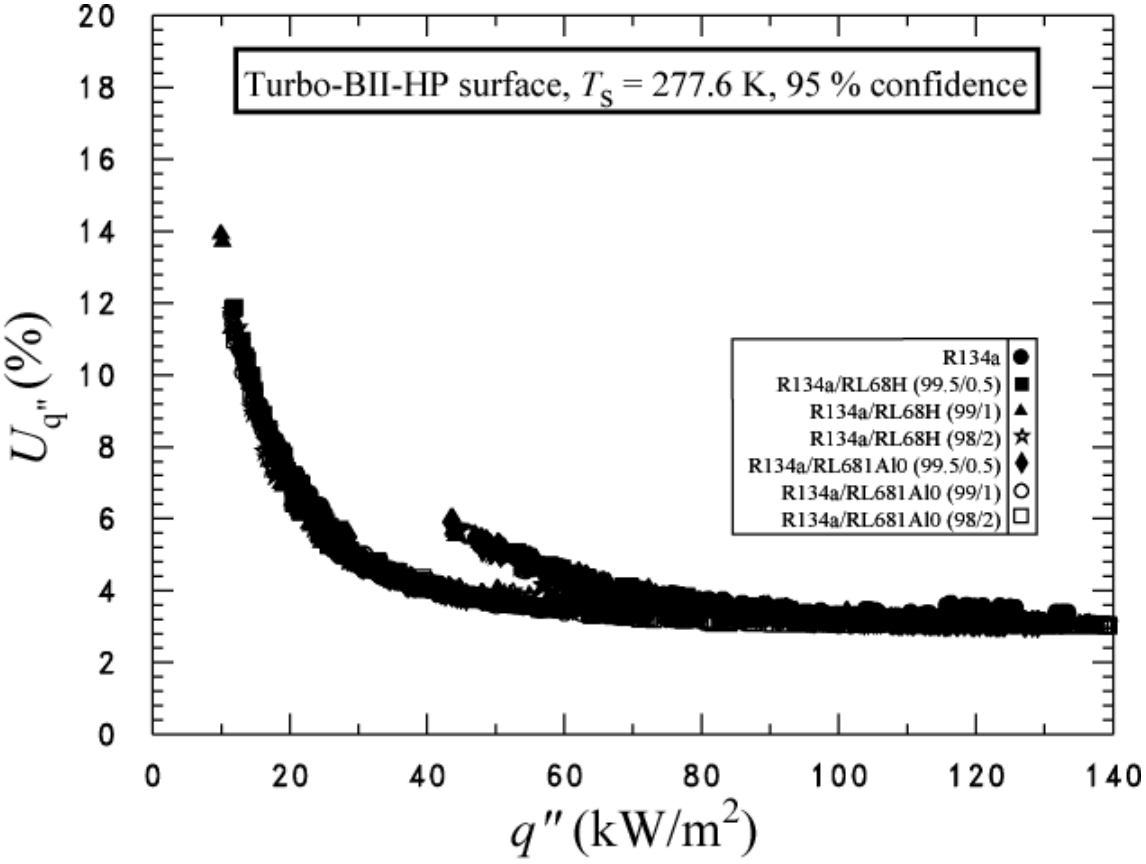

Fig. A.1 Expanded relative uncertainty in the heat flux of the surface at the 95 % confidence level

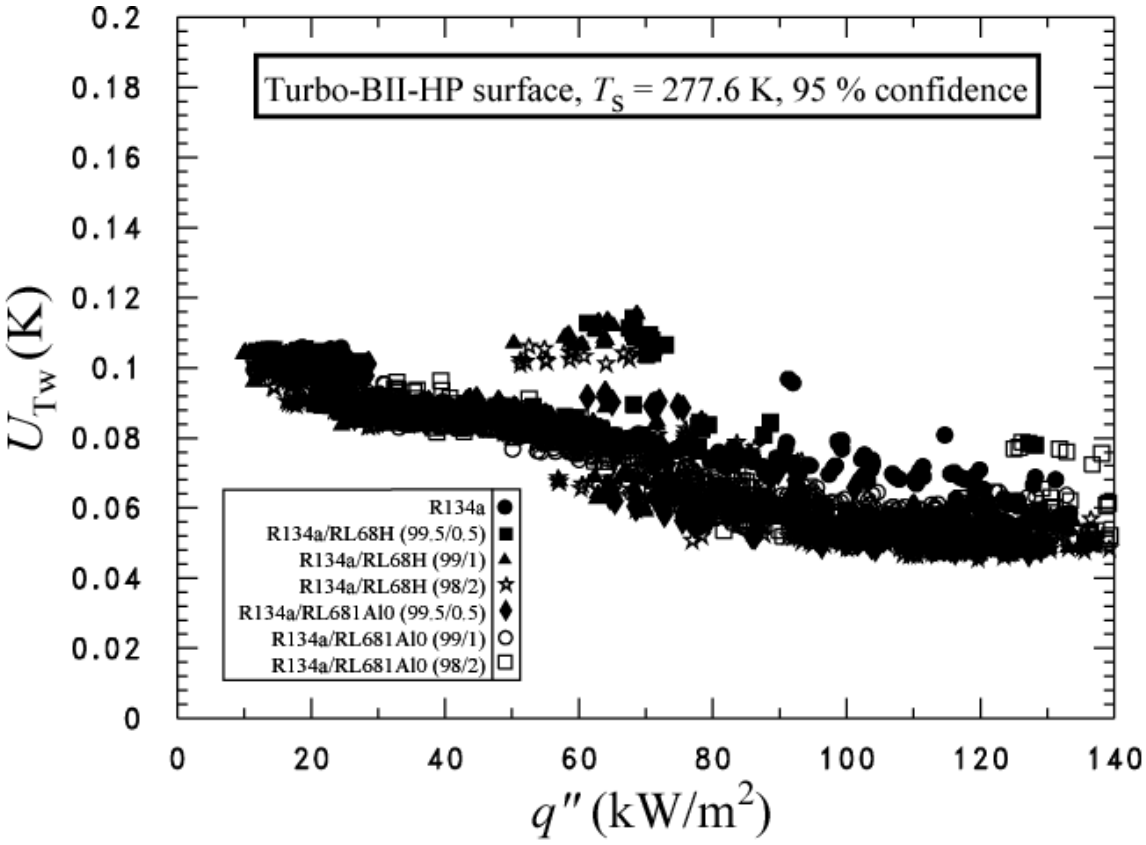

Fig. A.2 Expanded uncertainty in the temperature of the surface at the 95 % confidence level